1 Copper ions inhibit pentose phosphate pathway function in *Staphylococcus aureus*.

2

- 3 Javiera Norambuena¹, Hassan Al-Tameemi¹, Hannah M. Bovermann, Jisun Kim³, William
- 4 N. Beavers², Eric P. Skaar², Dane Parker³, Jeffrey M. Boyd^{1*}
- ¹Department of Biochemistry and Microbiology, Rutgers University, New Brunswick, New
- 6 Jersey, USA.
- ²Department of Pathology, Microbiology, and Immunology, Vanderbilt University Medical
- 8 Center, Nashville, Tennessee, USA.
- ⁹ Department of Pathology, Immunology and Laboratory Medicine, Center for Immunity
- and Inflammation, Rutgers New Jersey Medical School, Newark, New Jersey, USA
- 11 \$Present address: Department of Pathobiological Sciences, Louisiana State University,
- 12 Baton Rouge, Louisiana, USA.
- 13 *To whom correspondence may be addressed: Jeffrey M. Boyd, Department of
- 14 Biochemistry and Microbiology, Rutgers University, 76 Lipman Drive, New Brunswick,
- New Jersey, 08901, Telephone: (848) 932-5604, E-mail: jeffboyd@SEBS.rutgers.edu.

16

- 17 Running Title: The roles of Cu ions detoxification in S. aureus pathogenesis and
- 18 metabolism

19

Abstract

21

22

23

24

25

26

27

28

29

30

31

32

33

34

35

36

37

38

39

40

41

42

To gain a better insight of how Cu ions toxify cells, metabolomic analyses were performed in S. aureus strains that lacks the described Cu ion detoxification systems ($\triangle copBL$ $\triangle copAZ$; cop^{-}). Exposure of the cop^{-} strain to Cu(II) resulted in an increase in the concentrations of metabolites utilized to synthesize phosphoribosyl diphosphate (PRPP). PRPP is created using the enzyme phosphoribosylpyrophosphate synthetase (Prs) which catalyzes the interconversion of ATP and ribose 5-phosphate to PRPP and AMP. Supplementing growth medium with metabolites requiring PRPP for synthesis improved growth in the presence of Cu(II). A suppressor screen revealed that a strain with a lesion in the gene coding adenine phosphoribosyltransferase (apt) was more resistant to Cu. Apt catalyzes the conversion of adenine with PRPP to AMP. The apt mutant had an increased pool of adenine suggesting that the PRPP pool was being redirected. Overproduction of apt, or alternate enzymes that utilize PRPP, increased sensitivity to Cu(II). Increasing or decreasing expression of prs resulted in decreased and increased sensitivity to growth in the presence of Cu(II), respectively. We demonstrate that Prs is inhibited by Cu ions in vivo and in vitro and that treatment of cells with Cu(II) results in decreased PRPP levels. Lastly, we establish that S. aureus that lacks the ability to remove Cu ions from the cytosol is defective in colonizing the airway in a murine model of acute pneumonia, as well as the skin. The data presented are consistent with a model wherein Cu ions inhibits pentose phosphate pathway function and are used by the immune system to prevent S. aureus infections.

Author Summary

43

44 Antimicrobial resistance is a global health emergency. There is an increasing demand to develop new drugs and repurpose chemotherapeutics to prevent and treat infections. 45 46 Metals and metal ions have been used as effective antimicrobials for millennia. This 47 effectiveness is likely due to their ability to simultaneously inhibit multiple cellular 48 processes. Copper (Cu) is a metal that has been used by humans as a prophylactic. 49 Furthermore, the human immune system utilizes Cu to aid bacterial killing or growth 50 inhibition. The human pathogen Staphylococcus aureus has two described Cu ion 51 detoxification systems, underscoring the efficacy of Cu ions to negatively impact S. 52 aureus growth and survival. Questions remain about how bacteria are toxified by Cu ions. Understanding how Cu kills and inhibits bacterial growth will provide useful information 53 54 for designing and implementing antimicrobial chemotherapy to decrease bacteria burden. 55 Herein, we demonstrate that the essential enzyme Prs is a target of Cu ions in *S. aureus*. 56 Using mouse models of pneumonia and skin infections, we demonstrate that S. aureus 57 that cannot effectively remove Cu ions from the inside of the cell are defective in 58 colonizing tissues.

- 60 **Key Words:** Staphylococcus aureus, copper, PRPP, adenine phosphoribosyltransferase,
- 61 prs, pentose phosphate pathway, antimicrobial resistance

Introduction

Copper (Cu), in both its ionic and metallic forms, has been used as an antimicrobial for millennia. Several studies have demonstrated that bacterial strains that are genetically modified to have a decreased ability to remove Cu ions from their cytosols have decreased survival on copper or copper alloy surfaces [1-3]. A Cu ion probe was used to demonstrate that bacteria aid the release Cu ions from dry or moist metallic Cu metal surfaces which then accumulate in their cytosol [4]. These studies suggest that when bacteria contact metallic Cu surfaces, Cu ions are liberated, are mobilized to the cytosol, and contribute to killing.

Cu ions have significant roles in biology including acting as an enzymatic cofactor for redox reactions; however, an excess of intracellular Cu ions cause intoxication [5]. It has been shown that intracellular Cu ions can cause demetallation and/or mismetalation of proteins with solvent exposed metal-binding sites [6, 7]. Cu ions can disrupt iron-sulfur (FeS) clusters [6] resulting in Fe release which can potentiate oxidative stress [8]. Cu can also inhibit the maturation of FeS proteins by binding to synthesis and assembly factors [9-12]. Cu(I) and Fe(II) can catalyze the production of hydroxyl radicals resulting in oxidative stress which can damage biological polymers [13, 14]. Although, *in vivo*, cytosolic Cu ion accumulation does not appear to cause DNA damage, suggesting that ROS production is not a primary mechanism for Cu ion induced killing or growth inhibition [15].

Cu ions aid humans in preventing and clearing infections [16-18]. Cu ions accumulate at sites of inflammation [17], within macrophage intracellular vesicles [19], and in phagosomes [20] where they aid bacterial clearance [21]. *Staphylococcus aureus*

strains that have been genetically modified to be defective in exporting Cu from the cytosol have decreased survival in macrophages and whole blood [22, 23]. Proper Cu ion removal from the S. aureus cytosol was required for complete fitness in a murine model of urinary tract of infection [24].

To aid in the prevention of cytosolic Cu ion accumulation, *S. aureus* USA300 possess two Cu-exporting ATPases coded by *copA* and *copB*. CopA is a P1-type ATPase [25] and it is in an operon with *copZ*. CopZ binds Cu(I) and delivers it to CopA for export [26]. CopB is also a P1-type ATPase and it is in an operon with *copL* [5, 23]. CopL is an extracellular Cu ion binding lipoprotein that likely prevents the entry of Cu to the cytoplasm [5]. The *copBL* operon is coded within the ACME transposable element found in some S. aureus strains [27].

The mechanisms by which cytosolic Cu ion accumulation intoxicates bacterial cells appears to be multifaceted and it is not entirely clear which processes are inhibited resulting in cell death [10, 28-30]. For this study, we used a strain which lacks the described Cu detoxification systems ($\Delta copBL$ and $\Delta copAZ$; strain named cop) to analyze the effect of cytosolic Cu ion accumulation and to identify metabolic bottlenecks to predict enzymes or pathways that are inhibited [31]. Using unbiased approaches, we demonstrate that an inability to remove Cu ions from the cytosol results in defective function of the pentose phosphate pathway (PPP). Genetic data suggest that altering the pool of phosphoribosyl pyrophosphate (PRPP) modulates the sensitivity of *S. aureus* to growth in the presence of Cu(II). We also establish that Cu(I) poisons the enzyme phosphribosylpyrophosphate synthetase (Prs), which produces the essential metabolite

PRPP. Finally, we corroborated the importance of cytosolic Cu-detoxification systems in colonization of skin and airways using murine models of infection.

109
110

Results

Cu(II) treatment perturbs carbon flow through central metabolic pathways.

To better understand the effects of Cu(II) treatment on intracellular metabolite pools we performed unbiased metabolomic analyses on the *S. aureus cop*⁻ strain. We exposed an exponentially growing culture to 5 μ M Cu(II) for 30, 60, or 180 minutes while growing in tryptic soy broth (TSB). We picked this concentration of Cu(II) because it did not significantly affect the growth of the cop- strain and we previously demonstrated that this amount of Cu(II) was sufficient to cause cytosolic accumulation in the cop- strain compared to the WT [32]. Although the MIC for Cu (2 mM) is quite high for the cop- strain cultured in TSB, incubating with a concentration of Cu(II) significantly lower than 2 mM still retards growth. We utilized 5 μ M Cu(II) to ensure that any significant differences in metabolite concentration were the result of Cu ions and not a slow growth phenotype.

Metabolites that were significantly altered when compared to cultures treated with the vehicle control at each time point are listed in Table 1 and illustrated in Figure 1. The complete list of metabolite concentrations can be found in Table S1. The number of significantly altered metabolites was largest after 30 minutes of exposure and then decreased over time. These data suggest that the metabolic network of *S. aureus* is responsive to growth in the presence of Cu(II) and adapts to redirect metabolic flux to help buffer against the effects of Cu ions.

After 30 minutes of growth in the presence of Cu(II) there was a significant accumulation of the glycolytic metabolites glucose, glucose 6-phosphate, dihydroxyacetone phosphate, 3-phosphoglycerate (3PG) and fructose 6-phosphate. These metabolites are processed upstream of glyceraldehyde 3-phosphate

dehydrogenase (GapA) which was previously shown to be inhibited by Cu ions *in vivo* [33]. These metabolites would also be expected to accumulate if there was a Cu-induced bottleneck in the PPP (Figure 2A). Consistent with a block in the PPP, there was an increase in the accumulation of ribose 5-phosphate (R5P) and ribulose 5-phosphate (Ru5P) which are key metabolites of the pentose phosphate pathway. The only metabolite that accumulated in all three time points was R5P. Ru5P, serine, 3-phosphoglycerate, and dihydroxyacetone phosphate accumulated in two of the time points. These data are consistent with the hypothesis that Cu ion accumulation alters carbon flux through glycolysis and/or the PPP.

Carbon from glucose is fluxed through the pentose phosphate pathway.

We tested the hypothesis that carbon from glucose is fluxed through the PPP to metabolites requiring R5P synthesis when *S. aureus* is grown on TSB medium. We cultured cells in a label-free TSB medium to exponential growth phase and transferred cells to ¹³C₆-glucose TSB. Samples were taken at 15, 30 and 60 minutes after the switch and metabolites were quantified. After fifteen minutes ¹³C was incorporated into metabolites that are intermediates in glycolysis and the PPP pathways (Figure 2 and Table S2). This list of metabolites included R5P. There was also an increase in ¹³C in metabolites derived from R5P including purines and pyrimidines (Table 2). For many of the metabolites, the concentration of incorporated ¹³C atoms increased as a function of time (Figure 2). Likewise, the total amount of ¹³C atoms in the nicotinamide dinucleotides NADH and NAD+ increased over-time (Figure S1). In addition, the number of ¹³C atoms per individual NADH and NAD+ molecule increased over time. We were not able to

determine which atoms were labeled with ¹³C in the NAD⁺ or NADH (or any other molecule), but we did witness the formation of molecules that contained label in 12, 13, or 14 of the 21 total carbon atoms (five carbons from adenine, 6 from nicotinamide, 10 from ribose) suggesting that the ribose component was labeled with ¹³C from glucose.

Requiring carbon to be fluxed though the PPP increases sensitivity to Cu(II).

Either glucose or gluconate can be used to produce R5P. Glucose can be processed through glycolysis or the PPP; however, gluconate can only be processed through the PPP in *S. aureus* (Figure 2A). We hypothesized that if growth with Cu(II) results in decreased PPP function, *S. aureus* would have decreased growth when the primary carbon source was gluconate as compared to glucose. We spot plated the *cop* strain in the presence and absence of Cu(II) on defined media containing either glucose or gluconate as a primary carbon source (Figure 3A). Growth was similar if glucose or gluconate were primary carbon sources in the absence of exogenously supplied Cu(II); however, there was a more profound growth defect on gluconate medium when the media were supplemented with Cu(II). A similar trend was noted when cells were cultured in liquid defined media with either glucose or gluconate as primary carbon sources and various concentrations of Cu(II) (Figure 3B).

We next tested the hypothesis that decreasing flux from glucose into the PPP would increase the sensitivity of *S. aureus* to growth in the presence of Cu(II) when glucose was the primary carbon source. To this end, we created a *cop*⁻ strain with a lesion in the gene that encodes for 6-phosphogluconolactonase (*pglS*; SAUSA300_1902), which hydrolyzes 6-phosphogluconolactone to 6-P gluconate (Figure 2A). Growth on

gluconate as the primary carbon source should bypass the need for PgIS, whereas growth with glucose partially relies on PgIS to flux carbon from glucose into the PPP. It was previously demonstrated that conversion of 6-phosphogluconolactone to 6-P gluconate can occur spontaneously, making pgIS non-essential for growth with glucose [34]. We cultured the cop⁻ pgIS::Tn and cop⁻ strains on defined media with either glucose or gluconate as carbon source. The cop⁻ pgIS::Tn mutant grew similar to the cop⁻ strain in defined medium with gluconate as a carbon source, but had a slow growth phenotype when glucose was provided as a carbon source (Figure 3C) supporting a role for PgIS in PPP. Glucose is the primary carbon source is TSB. The cop⁻ and cop⁻ pgIS::Tn strains behaved similar when cultured on tryptic soy agar (TSA) medium; however, supplementation of the TSA medium with Cu(II) resulted in a significant growth defect in the cop⁻ pgIS::Tn strain when compared to the cop⁻ strain and the phenotype could be genetically complimented (Figures 3D and S2).

We further analyzed the necessity of a proper functioning PPP for Cu resistance using a strain lacking transketolase (Tkt). The $cop^-\Delta tkt::kan$ mutant strain had a small colony phenotype on TSA medium making it difficult to accurately compare the growth with that of the cop^- strain when cultured with Cu(II). Therefore, we determined the minimal inhibitory concentration (MIC) for Cu(II) when growing in TSB media. Whereas the MIC for Cu(II) was 2 mM for the cop^- strain, it was 1 mM for the cop-pglS::Tn and $cop-\Delta tkt::kan$ strains. Taken together, these data suggest that perturbing carbon flux though the PPP alters the sensitivity of *S. aureus* to Cu(II).

Suppressor analysis suggests that sparing PRPP protects against Cu(II) intoxication.

We generated a transposon mutant library in the *cop*⁻ background. The library was plated on TSA medium containing 2.5 mM Cu(II) which is a non-permissive growth concentration of Cu(II) for the *cop*⁻ strain. Transposon insertions that led to suppression of the Cu(II) sensitivity phenotype of the *cop*⁻ strain were mapped to three genes: *mntA*, *ispA*, and *apt*. We previously described a role for MntABC in Cu(II) resistance [31]. The two *apt::Tn* insertions were located at the TA/AT site located at +438 (*apt::Tn*). The *apt* gene is downstream of *recJ*, in an apparent operon. The role of *ispA* in Cu ion homeostasis is unknown and not the focus of this study.

To verify the function of Apt (SAUSA300_1591) in protecting against Cu(II) intoxication, we created an Δapt::tetM cop⁻ strain. The Δapt::tetM mutation provided resistance to Cu(II) when compared to the cop⁻ strain in solid or liquid media containing Cu(II) (Figures 4A and S3). Since apt appears to share a promoter with recJ, we cloned apt into a vector (pEPSA5) that placed it under a non-native promoter (xyIRO). Introduction of the pEPSA5_apt vector into the cop⁻ apt::Tn or cop⁻ Δapt::tetM strain returned growth to that of the cop⁻ strain containing empty vector when Cu(II) was present (Figure 4B). Note that it was not necessary to induce expression of apt and the basal "leaky" expression was sufficient to compliment the mutants.

We next tested the hypothesis that the absence of Apt has no effect in intracellular Cu accumulation. To this end, the $cop^-\Delta apt::tetM$ and cop^- strains were cultured in TSB for 8 hours before adding 5 μ M Cu(II) and incubated for an additional 60 minutes. We determined the concentration of cell associated Cu using ICPMS analysis and

standardized the amount of Cu associated with the cells to the concentration of magnesium or sulfur. Both strains accumulated the same amount of Cu (Figure S4).

The iron-sulfur cluster containing dehydratase aconitase (AcnA) is inactivated by Cu(I) [6]. We previously found that strains that have decreased Cu ion uptake protected AcnA from Cu(I) poisoning. The absence of Apt did not alter the sensitivity of AcnA to Cu ions which is consistent with the ICPMS data in suggesting that the lack of Apt does not alter Cu ion uptake or intracellular Cu ion accumulation (Figure S5). Taken together, these data led to the hypothesis that the absence of Apt reroutes metabolism to promote Cu(II) resistance.

The *apt* gene is predicted to code for an adenine phosphoribosyltransferase that functions in purine salvage [35]. Apt catalyzes the conversion of adenine (or guanosine) and phosphoribosyl pyrophosphonate (PRPP) to AMP (or GMP) and pyrophosphate [35]. We used untargeted metabolomic analysis to examine whether Apt functioned in adenine homeostasis in *S. aureus*. The *cop⁻* Δ*apt::tetM* strain accumulated 10-fold more adenine than the *cop⁻* strain verifying a role for Apt in adenine homeostasis (Figure 4C, Table 3, and Table S3). The *cop⁻* Δ*apt::tetM* strain had decreased accumulation of metabolites of the pentose phosphate pathway (R5P, sedoheptulose), purine precursors (AICAR, AICAriboside), and pyrimidines (dUMP, cytosine) verifying that it's absence is results in a metabolic reprograming of nucleotide metabolism.

Genetic evidence suggests that modulating PRPP levels alters growth in the presence of Cu(II)

We hypothesized that increasing Apt activity would decrease PRPP levels resulting in increased sensitivity to Cu(II). To this end, we overexpressed *apt* using pEPSA5_*apt* and added xylose to induce expression. The *cop*⁻ strain containing pEPSA5_*apt* was significantly more sensitive to Cu(II) than the *cop*⁻ strain containing the empty vector (pEPSA5) (Figures 5A and S6).

248

249

250

251

252

253

254

255

256

257

258

259

260

261

262

263

264

265

266

267

268

269

270

In S. aureus, there are nine enzymes that utilize PRPP as a co-substrate (Table 4) [36-38]. We hypothesized that overproduction of any enzyme that utilizes PRPP will increase in Cu(II) sensitivity. We created eight plasmid vectors (including the apt clone) using pEPSA5 that allowed us to induce transcription of the individual genes. When cultured on TSA with xylose, none of the strains over-producing PRPP utilizing enzymes displayed a growth phenotype. However, if TSB medium was supplemented with Cu(II) and xylose, strains over-producing apt, upp, htp, hisG, purF, or SAUSA300 1894 displayed worse growth than the cop⁻ strain carrying the empty vector (Figure 5A). Overproduction of *purE* or *pyrE* did not alter growth in the presence or absence of Cu(II) in TSB medium. However, when cultured on defined medium supplemented with hypoxanthine (HPX) or orotate, the co-substrates for PurE, the cop- strain overexpressing purE was sensitized to Cu(II) (Figure 5B and S7A). Likewise, the inclusion of HPX in the presence of Cu(II) increased the growth defect of the strain over-expressing hpt (Figure S7B). Adding the substrates for SAUSA300 1804 (nicotinate), Upp (uridine), or Apt (adenine) sensitized the cop- strains to growth in the presence of Cu(II) (Figure S7). For these experiments we did not add xylose to the growth media and relied on the "leaky" xyIRO promoter, which is why there is less of an effect with Cu(II) where compared to the data displayed in Figure 5A.

We tested the hypothesis that providing metabolites that require PRPP for synthesis will improve growth in the presence of Cu(II). We supplemented defined growth medium with uridine, tryptophan, guanosine, and nicotinamide mononucleotide (NMN) which have been shown to partially bypass the need for PRPP synthesis [39]. The addition of these compounds did not have a significant effect on the growth of the *cop*-strain in the absence of Cu(II); however, the presence of these compounds improved growth of the *cop*-strain if the medium was supplemented with Cu(II) (Figures 5C and S8).

Altering *prs* expression modulates sensitivity to Cu(II)

Prs phosphorylates R5P using ATP to produce PRPP and AMP [36]. The findings that R5P accumulated upon growth with Cu(II) and that altering PRPP levels changed sensitivity to Cu(II) suggested that Prs is inhibited by Cu ions. Increasing or decreasing the abundance of an enzyme can increase or decrease resistance to an inhibitor, respectively [40, 41]. We tested the hypothesis that modulating *prs* expression will alter the Cu(II) sensitivity phenotype of the *cop*⁻ strain.

We developed a plasmid based CRIPSRi system that utilizes the "dead" Cas9 (dCas9) from *Streptococcus pyogenes* to decrease the transcription of genes [42, 43]. We used pSK as the vector backbone, which is a low copy plasmid in *S. aureus* [44]. The guide RNAs were constitutively expressed and *dcas9* was under the transcriptional control of *tetRO*. We chose two different regions on *prs* that contain PAM sequences to target with guide RNAs (*prs1* and *prs2*). We included two control strains for the experiment. The first control strain contained a vector with a guide RNA that was not

homologous to the USA300_LAC genome [43] and the other with a guide RNA targeted to *hla*, which codes for alpha hemolysin [43].

The *cop*⁻ strain containing the CRISPRi system with guide RNAs specific to *prs*, *hla*, or the non-homologous guild RNA were plated on TSB media with or without 100 ng mL⁻¹ anhydrotetracycline (Atet). Plating with Atet resulted in death of the *cop*⁻ strains containing the *prs* guide RNAs but not the strains containing the *hla* or non-homologous guide RNAs (Figure S9). These data are consistent with previous studies suggesting that *prs* being an essential gene in *S. aureus* [45].

We next plated the strains on TSA containing a lower concentration of Atet as to decrease the stringency of the CRISPRi-based inhibition and examined sensitivity to growth with Cu(II). When Atet was included in the medium, the *cop*⁻ strains containing the *prs* guide RNAs displayed a hyper-sensitivity to growth in the presence of Cu(II) when compared to the *cop*⁻ strains containing the *hla* guide RNA or the empty vector (Figure 6A). The concentration of Atet utilized did not result in a growth defect on TSB medium and the concentration of Cu(II) included did not result in cell death if Atet was not included.

Two experiments were used to ensure that our CRIPRi system was working properly. First, we spot plated the *cop*⁻ strain containing the *hla*, *prs*, or non-homologous guide RNAs on TSA media containing 5% rabbit blood. The addition of Atet resulted in decreased hemolysis in the strain containing the *hla* guide RNA but not the strains expressing the *prs1* or non-homologous guild RNAs (Figure S10A). We next quantified RNA transcripts corresponding to *hla* and *prs*. The *hla* and *prs* transcripts were significantly decreased upon induction with Atet in strains containing the corresponding guide RNAs (Figures 6B and S10B).

We increased the gene dosage of *prs* by placing it under the transcriptional control of *xyIRO* using pEPSA5. For these experiments we did not add xylose to the growth media and relied on the "leaky" *xyIRO* promoter for expression. The *cop*- strain containing pEPSA5_*prs* grew more proficiently than the *cop*- strain containing pEPSA5 on solid or liquid media medium containing Cu(II) whereas there was not an effect on TSB medium (Figures 6C and S6). We included the *cop*- strain containing pEPSA_*apt* as a control. Taken together, these data are consistent with the hypothesis that increasing or decreasing *prs* transcription results in hypo- and hyper-sensitivity to Cu(II) in the growth media, respectively.

Copper inhibits Prs

We tested the hypothesis that Cu ions inhibit Prs. To measure Prs activity we used a coupled assay in which the AMP produced from the ATP-dependent phosphorylation of R5P is measured using an NADH-coupled enzyme system [46]. This assay was unable to detect an increase in R5P-dependent AMP production (above background levels) in cell-free lysates generated from the *cop*⁻ strain. To circumvent this problem, we utilized the *cop*⁻ strain containing pEPSA5_*prs* which allowed us to over-produce Prs. Uncoupling *prs* transcription from its native promoter also decreased the likelihood that growth in the presence of Cu(II) alters *prs* promoter activity. R5P-dependent AMP production could be detected in cell-free lysates generated from the *cop*⁻ pEPSA5_*prs* strain (Figure 7A). We next monitored Prs activity in the *cop*⁻ pEPSA5_*prs* strain after growth in TSB-xylose media the presence or absence of Cu(II). The R5P-dependent AMP generation was decreased by 40% in cell lysates from cells that were exposed to 5 µM Cu(II) (Figure 7A).

We tested the hypothesis that PRPP levels would be decreased upon growth in the presence of Cu(II). We cultured the *cop-* and *cop-* $\Delta apt::tetM$ strains in the presence and absence 5 μ M Cu(II) and quantified PRPP levels in cell-free lysates. PRPP levels were approximately 50% in the *cop-* strain co-cultured with Cu(II) (Figure 7B). Surprisingly, the PRPP levels in the *cop-* $\Delta apt::tetM$ strain were the same as found in the *cop-* strain and addition of Cu(II) had no effect on PRPP levels, suggesting a mechanism for how the null apt mutations suppress the Cu resistance of the cop^- strain.

We next purified recombinantly produced Prs and assessed activity in the presence and absence of Cu ions. Once Cu(II) enters the cytosol it interacts with thiol containing compounds which aid its reduction to Cu(I) [6, 47]. The addition of 2 μ M Cu(I) resulted in a 7-fold decrease in Prs activity and activity could not be detected after the addition of 5 μ M Cu(I) (Figure 7C). The addition of 5 μ M Cu(II) did not result in a significant decrease in Prs activity. We left Prs out of the assay mix and examined the effect of 5 μ M Cu(I) on the coupling enzyme mixture. Cu(I) did not inhibit AMP-dependent NADH oxidation, suggesting that, at the concentrations tested, the Cu(I) ions were not significantly inhibiting the coupling enzymes, but rather inhibiting Prs (Figure S11).

Removing host derived Cu ions from the cytosol is important for pathogenesis.

Work by others has demonstrated that effective removal of Cu ions from the cytosol is important for survival when challenged with human blood or macrophages [22]. Macrophages play an important role in clearing *S. aureus* from lung and bronchoalveolar lavage fluid, and thereby, protect against infection [48, 49]. We examined the pathogenesis phenotypes of the *cop*⁻ strain and the individual copper-export mutants in a

murine model of acute pneumonia. A small but insignificant decrease in bacteria in the BALF was observed with the $\triangle copBL$ mutant. A 58% reduction in bacterial burden in BALF was detected with the $\triangle copAZ$ strain, while the cop^- strain saw a 91% reduction (P<0.0001; Figure 8A). This pattern of clearance was also observed in lung tissue (Figure 8B). Significantly fewer neutrophils, eosinophils, and NK cells were detected in the BALF, likely due to the reduced bacterial burden (Figure 8C). The attenuation of the cop^- strain was further confirmed in a murine model of skin and soft tissue infection. By day 5 of infection, the cop- strain had 78% less (Figure 8D) bacteria than the WT strain. These data confirm the important role Cu detoxification plays in the pathogenesis of *S. aureus* infection.

Discussion

The inhibition of enzymes by Cu ions has been demonstrated, but mechanism(s) by which Cu ions kill or inhibit the growth of bacteria remains unknown and is likely multifaceted. Because of this, it has been difficult for researchers to identify a single cellular target that when inhibited by Cu results in cell death or growth inhibition. It was demonstrated that Cu(I) can cause the displacement of solvent accessible FeS clusters in proteins, such as certain SAM radical proteins or dehydratases, yielding an inactive catalyst in enzymes that require the cofactor for function [6, 50]. However, the roles of the described dehydratases and SAM-radical enzymes can be bypassed by growth in a rich medium such as Luria-Bertani broth.

Additional work in *E. coli* suggests that the A-type FeS cluster carriers SufA and IscA, as well as the FeS cluster synthesis scaffold IscU, bound Cu(I) *in vivo* and are likely inhibited in FeS protein assembly and/or synthesis when associated with Cu [9, 11]. *E. coli* utilizes two FeS cluster synthesis systems, ISC and SUF, that share a degree of functional, but not biochemical, redundancy [51]. The deletion of both *sufA* and *iscA* is synthetically lethal [52]. Therefore, complete inhibition of the functions of SufA and IscA (or ErpA) by Cu(I) should result in death. *S. aureus* utilizes the SUF system to synthesize FeS clusters [53]. Deletion of *sufA* has little to no measurable impact on *S. aureus* fitness suggesting that Cu ion inhibition of A-type scaffold is not lethal [54].

Additional described effects of Cu ions on physiology may include ROS generation, inhibition of cytochrome oxidase, and increasing protein aggregation. Imlay and colleagues have presented evidence that cytosolic Cu ions likely do not directly contribute to ROS generation in *E. coli* [15]. Cytochrome oxidases are not essential in *S. aureus*

[55]. It was recently demonstrated that when *E. coli* is cultured anaerobically in the presence of Cu(I) ions there is an increase in protein aggregation under anaerobic growth [56]. The authors did not report significantly increased protein aggregation during aerobic growth conditions and at low copper concentrations, such as those described in this study.

We demonstrate that there is a large variation in the amount of Cu(II) that is required to inhibit growth of the *cop*⁻ strain if the media is varied. Low µM concentrations of Cu(II) are required for growth inhibition in chemically defined media whereas mM concentrations are required in complex media. Defined media contains fewer molecules, such as amino acids, that can interreact with metal ions including Cu in making the Cu ions more bioavailable [57]. In addition, Cu ions interrupt numerous metabolic processes (glycolysis, pentose phosphate pathway, TCA cycle, FeS cluster synthesis, etc.) and metabolites present in complex media may allow for bypass of some of these metabolic bottlenecks.

The data presented herein support a model where growth in the presence of Cu ions results in the inhibition of the essential enzyme Prs (Figure 9). In support of this model, glycolytic and PPP metabolites accumulate upon Cu(II) treatment, whereas PRPP levels decrease. Physiological or genetic alterations that vary carbon flux though the PPP altered sensitivity to Cu(II). Modulating PRPP pools or bypassing the need for PRPP synthesis by adding metabolites that require PRPP for synthesis altered sensitivity to Cu(II). Increasing or decreasing *prs* expression improved and impaired growth with Cu(II), respectively. Lately, Prs activity was decreased in cell lysates after growth with Cu(II) and Prs was inhibited in vitro by Cu(I).

It is currently unclear how Cu(I) is inhibiting Prs. Prs does require a divalent metal and it prefers Mg(II) or Mn(II) [36]. It was reported that Ca(II) acts as an inhibitor of the Salmonella enterica Prs by preventing Mg(II) binding [36]. Similar as reported here, Prs was not inhibited by Cu(II) in vitro, but the authors did not examine Cu(I) [58]. We note that there is a conserved histidine residue in the active site of Prs that is utilized for coordinating the ribose [59, 60]. We theorize that Cu(I) inactivates Prs by blocking active site access or by mismetalating the enzyme, and we plan to test these hypotheses in the future.

This manuscript complements a previous study demonstrating that Cu ions inhibit glyceraldehyde 3-dehydrogenase (GapDH) [61]. A proteomic study found that several enzymes involved in glycolysis and the PPP (ex. Fda, GapA, Tkt) had increased abundances upon growth with Cu(II). It is likely that these alterations were the result of Cu ions altering the ability to flux carbon through these pathways. The only two operons in *S. aureus* strain LAC that that been demonstrated to respond to the Cu-dependent transcription factor CsoR are *copAZ* and *copBL* suggesting that the altered expression of the genes that encode these metabolic enzymes are not responding directly to the presence of Cu [62, 63]. Studies have found that GapA binds to Cu ions *in vivo* and *in vitro* [61, 64]. The metabolomic data presented here found that several glycolytic intermediates were increased when cells were cultured with Cu(II) for 30 minutes. We also noticed accumulation of 3-phosphoglycerate which is the product of GapA suggesting that there maybe also metabolic bottleneck downstream of GapA. Glyceraldehyde 3-phosphate, fructose 6-phosphate, and glucose 6-phosphate are

shared metabolites between glycolysis and PPP, so, it would be expected that there would be altered abundances of these metabolites if PPP function was decreased.

442

443

444

445

446

447

448

449

450

451

452

453

454

455

456

457

458

459

460

461

462

463

464

Cu ions are used by human macrophages to enhance bacterial clarence and several studies have highlighted the importance for proper Cu ion detoxification for S. aureus pathogenesis [21]. For the most part, studies have examined the role of the second horizontally transferred Cu(I) detoxification system CopBL transporter which is ubiquitous in USA300 linage. The copBL operon is encoded in the ACME transposable element [27]. Zapotoczna et al. examined the role of the copBL for survival when challenged with macrophages. S. aureus lacking CopB or CopL had significantly decreased survival in murine macrophages whereas a copA mutant had similar survival as the parent strain. It was also demonstrated that a strain carrying an allele of csoR (CHC strain) that encode a protein with decreased capability to respond to Cu(I) has decreased ability to survive in mouse macrophages affirming the importance of detecting and responding to Cu. The authors also noted an increased ability of a strain with two copper detoxification systems to survive in human whole blood. Likewise, the CHC strain showed decreased whole blood survival compared to the wild-type strain [22]. In a separate study, Purves et al. demonstrated that $\triangle copB$ or $\triangle copL$ strains had decreased survival in murine macrophages [23]. The concentration of Cu was elevated in urine from patients experiencing an infection of the urinary tract [24]. Using a murine urinary tract model of infection, the WT strain was competed against a $\triangle copB$ or $\triangle copL$ mutant and determined that both genes contribute to fitness. The $\triangle copB$ mutant had decreased colonization of urinary tracts compared to the parental strain [24]. The studies presented herein did not discern a phenotype for the $\triangle copBL$ mutant in the lungs or the BALF;

however, our findings did highlight a role for *copAZ* and the general export of Cu ions in lung pathogenesis. Moreover, we determined that Cu detoxification has a role in survival in a skin model of infection.

The data presented in this manuscript improves our knowledge of how intracellular Cu ions toxify cells. It also provides a mechanism by which Cu ions inhibit the growth of *S. aureus*. We demonstrated that Cu ion detoxification is necessary for survival in murine BALF and lung tissue in a pneumonia model of infection, as well as in a murine model of skin and soft tissue infection. We have devised a working model wherein Cu(I) inhibits PPP function resulting in decreased levels of the essential metabolite PRPP (Figure 9). It is yet to be determined whether the inhibition of the PPP by Cu ions is resulting in a decreased capability of *S. aureus* to cause infection.

Materials and Methods

Chemicals and bacterial growth conditions

All bacterial strains used for the studies were derived from the community associated *S. aureus* MRSA strain USA300_LAC [65]. Strains were grown at 37 °C in tryptic soy broth (TSB) (MP Biomedicals) or a chemically defined medium containing 11 mM glucose or 11 mM gluconate as a primary carbon source [66]. Solid tryptic soy (TSA) or chemically defined media was generated by adding 1.5% (weight/vol) agar (VWR). Liquid cultures were shaken at 200 rpm. Chelex-treated TSB was prepared as previously described [31]. Unless stated otherwise, cells were cultured in 10 mL capacity culture tubes containing 1.5 mL of liquid medium. The restriction minus strain *S. aureus* RN4220 was used for transformation [67] and transductions were done using bacteriophage 80α [68]. All *S. aureus* strains (Table 5) used in this study were derived from the $\Delta copAZ$ $\Delta copBL$ mutant (cop^- strain) [31]. *Escherichia coli* DH5 α was used for plasmids preparation (NEB) and *E. coli* BL21 was used for protein purification. Both were cultured in lysogeny broth.

Antibiotics were added at the final following concentrations: 100 μg mL⁻¹ ampicillin (Amp); 50 μg mL⁻¹ Kanamycin (Kan); 10 μg mL⁻¹ chloramphenicol (Cm); 10 μg mL⁻¹ to select for plasmids and 3.3 μg mL⁻¹ to maintain plasmids; erythromycin (Erm); 3 μg mL⁻¹ tetracycline (Tet); 3-100 ng mL⁻¹ anhydrotetracycline (Atet). The defibrinated rabbit blood agar plates were made as previously described [69]. The CuSO₄ was prepared in deionized and distilled water and filter sterilized. Protein concentrations were determined using Bradford reagent (Bio-Rad Laboratories Inc., Hercules, CA). Molecular reagents

were purchased from New England Biolabs, unless otherwise stated. Unless stated otherwise, all chemicals were purchased from Sigma-Aldrich (St. Louis, MO). DNA was sequenced at Azenta (South Plainfield, NJ).

503

504

505

506

507

508

509

510

511

512

513

514

515

516

517

518

519

520

521

522

500

501

502

Metabolomic analyses and PRPP measurements

Metabolomics. All metabolic analyses were conducted using biological triplicates. Overnight cultures (cop⁻ or cop- apt::tet) were diluted into fresh TSB to OD₆₀₀ 0.1, grown until OD₆₀₀ of 0.5 in a flask. At this point, 5 mL of culture was transferred to individual 30 mL capacity culture tubes and exposed to 0 or 5 µM Cu(II) for three hours. Samples for the metabolite profiling were prepared described previously [70]. Briefly, 1 mL of the cells pelleted, washed once with PBS, and resuspended in 1 mL of were Methanol: Acetonitrile: Water (2:2:1) solution. Cells were lysed by bead beating (2 cycles, 40 s each, 6.0 m s-1) using a FastPrep homogenizer (MP Biomedicals) and 0.1-mm silica glass beads (MP Biomedicals). Samples were centrifuged twice at 14,500 rpm at 4 °C for 2 minutes and supernatant retained. The supernatant was filtered with nylon membrane syringe filters (13 mm, 0.22 µm, Fisherbrand) and samples were store at -80 °C until metabolite analysis was performed.

Samples were analyzed at the metabolomics core of the Cancer Institute of New Jersey. HILIC separation was performed on a Vanquish Horizon UHPLC system (Thermo Fisher Scientific, Waltham, MA) with an XBridge BEH Amide column (150 mm × 2.1 mm, 2.5 µm particle size, Waters, Milford, MA) using a gradient of solvent A (95%:5% H₂O:acetonitrile with 20 mM acetic acid, 40 mM ammonium hydroxide, pH 9.4) and solvent B (20%:80% H₂O:acetonitrile with 20 mM acetic acid, 40 mM ammonium

hydroxide, pH 9.4). The gradient was 0 min, 100% B; 3 min, 100% B; 3.2 min, 90% B; 6.2 min, 90% B; 6.5 min, 80% B; 10.5 min, 80% B; 10.7 min, 70% B; 13.5 min, 70% B; 13.7 min, 45% B; 16 min, 45% B; 16.5 min, 100% B; and 22 min, 100% B. The flow rate was 300 µL min⁻¹. The column temperature was set to 25 °C. The autosampler temperature was set to 4 °C, and the injection volume was 5 µL. MS scans were obtained in negative mode with a resolution of 70,000 at m/z 200, in addition to an automatic gain control target of 3 x 106 and m/z scan range of 72 to 1000. Metabolite data was obtained using the MAVEN software package [71] (mass accuracy window: 5 ppm). The data from these experiments are included as Tables S1 and S3.

Carbon labeling experiments were performed using D-Glucose-¹³C₆ (389374, Sigma-Aldrich) using the *cop*⁻ strain. Overnight cultures were diluted to an OD₆₀₀ of 0.1 in 1.5 mL of fresh glucose-free TSB supplemented with 11 mM glucose in 10 mL capacity culture tube. Cells were cultured to an OD₆₀₀ of 0.5 cells, pelleted, washed twice with PBS, and resuspended in 1.5 mL of glucose-free TSB supplemented with 11 mM ¹³C₆ glucose. Cells were cultured for 15, 30 or 60 additional minutes before samples were collected and metabolites were extracted as described above. The data from these experiments is included as Table S2.

PRPP quantification. The cop⁻ and cop- apt::tetM strains vector were grown O.N. in TSB and diluted to an OD₆₀₀ of 0.1 in TSB medium. Cells were cultured until an OD₆₀₀ of 0.5 and 0 or 5 μM Cu(II) was added. Cells were cultured for an additional three hours before collecting 0.5 mL of cells and washing them with PBS. Cells were resuspended in 1 mL of PBS and lysed by bead beating using 0.1-mm silica glass beads (MP Biomedicals) as previously described [72]. Cell debris was removed by centrifugation 4°C

using a tabletop microcentrifuge. PRPP levels were measured using the PRPP ELISA Kit (Mybiosource) following manufacture instructions. PRPP levels were standardized to protein concentration which was determined using Bradford reagent.

Protein purification and enzymatic assays

Prs purification. An overnight culture of *E. coli* BL21 carrying pGEX-6P-1_prs was sub-cultured to OD₆₀₀ of 0.1 into LB-AMP medium. Cells were cultured for 1.5 hours at 37 °C and 0.1 mM IPTG was added. Cells were cultured for four more hours before harvesting by centrifugation. Cell pellets were washed with PBS and cells were resuspended in lysis buffer (50 mM phosphate buffer pH 7.5, 100 mM NaCl, 0.01 mg mL⁻¹ DNase and 1 mg mL⁻¹ lysozyme). Cells were lysed by sonication (Vibra-Cell; Sonics, Newtown, CT) on ice for 20 min at 40% (1s on / 1s off pulse). Cell debris was removed by centrifugation and supernatant was filter through a 0.22 µm polypropylene filter before loading onto GSTrap 4B Columns (Millipore Sigma). Protein was purified according to manufactures instructions. Purified Prs was dialyzed five times in a 1:1000 ratio (protein:buffer) against dialysis buffer (50 mM phosphate buffer, 150 mM NaCl, pH 7.5) at 4°C before use.

Aconitase activity assay. Cells were prepared as previously described [31]. Aconitase activity was measure as previously described [73] using a using Cary 60 UV-Vis spectrophotometer (Agilent, Santa Clara, CA).

Prs activity assays. For in vivo assays, the cop⁻ strain carrying the pEPSA5_prs vector was cultured overnight in TSB-Cm. The was then diluted to an OD₆₀₀ of 0.1 in 1.5 mL of TSB-Cm supplemented with 0.5% xylose. Cultures were grown as indicated for

metabolomics, one mL of cells were collected by centrifugation, and washed twice with PBS. Cells were resuspended in 1 mL of PBS and lysed by bead beating using 0.1-mm silica glass beads (MP Biomedicals). Cell debris was removed by centrifugation 4 °C using a tabletop microcentrifuge and supernatants were concentrated using Vivaspin 500 (3,000K MWCO, PES, Sartorius). Prs activity was measured by monitoring AMP formation using a coupled enzyme system [46]. For each extract, we subtracted the basal NADH oxidation activity (before addition R5P) from the R5P-dependent NADH oxidation. This was necessary due to the presence of many other enzymes that consume ATP and produce AMP. Measurements were carried out using UV-STAR® microplates (Greiner Bio-One) and Varioskan LUX Multimode Microplate Reader (Thermo Scientific). *in vitro* Prs activity assays contained 0.07 mg mL-1 Prs. Cu(I) was prepared using asorbic acid as previously described [74].

Murine infection assays

C57BL/6 mice, 6 weeks of age, were intranasally infected with 2-4 x 10^7 cfu of *S. aureus* in 50 µL of PBS under anesthesia (ketamine and xylazine). Bacterial loads were enumerated at 24 h post infection from bronchoalveolar lavage fluid (BALF) by washing the airway 3 times with 1 ml of PBS and homogenized lung tissue. Skin infection was initiated with 2-4 x 10^6 cfu of *S. aureus* in 100 µL of PBS delivered subcutaneously. Flow cytometry was performed on fluorescently labelled cell from BALF as described previously [75]. Bacterial counts were quantified by using CHROMagar *S. aureus* plates (BD Biosciences).

Ethics statement

Animal work in this study was carried out in strict accordance with the recommendations in the Guide for the Care and Use of Laboratory Animals of the NIH (National Academies Press, 2011), the Animal Welfare Act, and US federal law. Protocols were approved by the Institutional Animal Care and Use Committee of Rutgers New Jersey Medical School of Newark, New Jersey, USA.

Statistical analysis

One-way ANOVA followed by a Dunnet test analysis was performed for multiple group comparison to a control. For two group comparisons (controls vs treatment or between bacterial strains), student's t-tests were performed. Multiple group comparisons for animal data were performed using an ANOVA with a Kruskal-Wallis test or a Mann-Whitney non-parametric test for two group comparisons. All analyses were conducted with Sigmaplot 11, Microsoft, Excel, or Prism 9.

Financial Disclosures

This work was supported by NIAID 1R01AI139100-01, NSF 1750624, and USDA MRF project NE-1028 to JMB. The Skaar lab is funded by grants R01AI150701, R01AI138581, and R01AI145992 from the NIH. The Parker lab is funded by NIH grant R21AI153646, New Jersey Health Foundation grant PC 142-22 and the New Jersey Commission on Cancer Research COCR22RBG005. The funders had no role in this study. JN, JK, WB, received salary from the NIH through the grants listed above.

615 Figures Legends

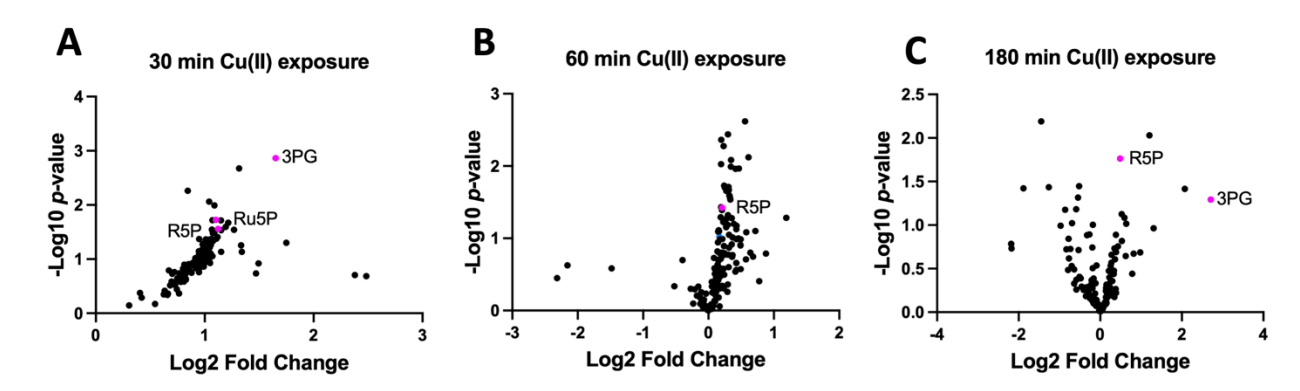


Figure 1. Growth with Cu(II) alters metabolite pools. Volcano plots of Log₂ fold change of metabolite abundances isolated from *cop*⁻ cells after 30 (panel A), 60 (panel B), and 180 (panel C) minutes after the addition of Cu(II) to the growth media. Data represent the average of three biological replicates.

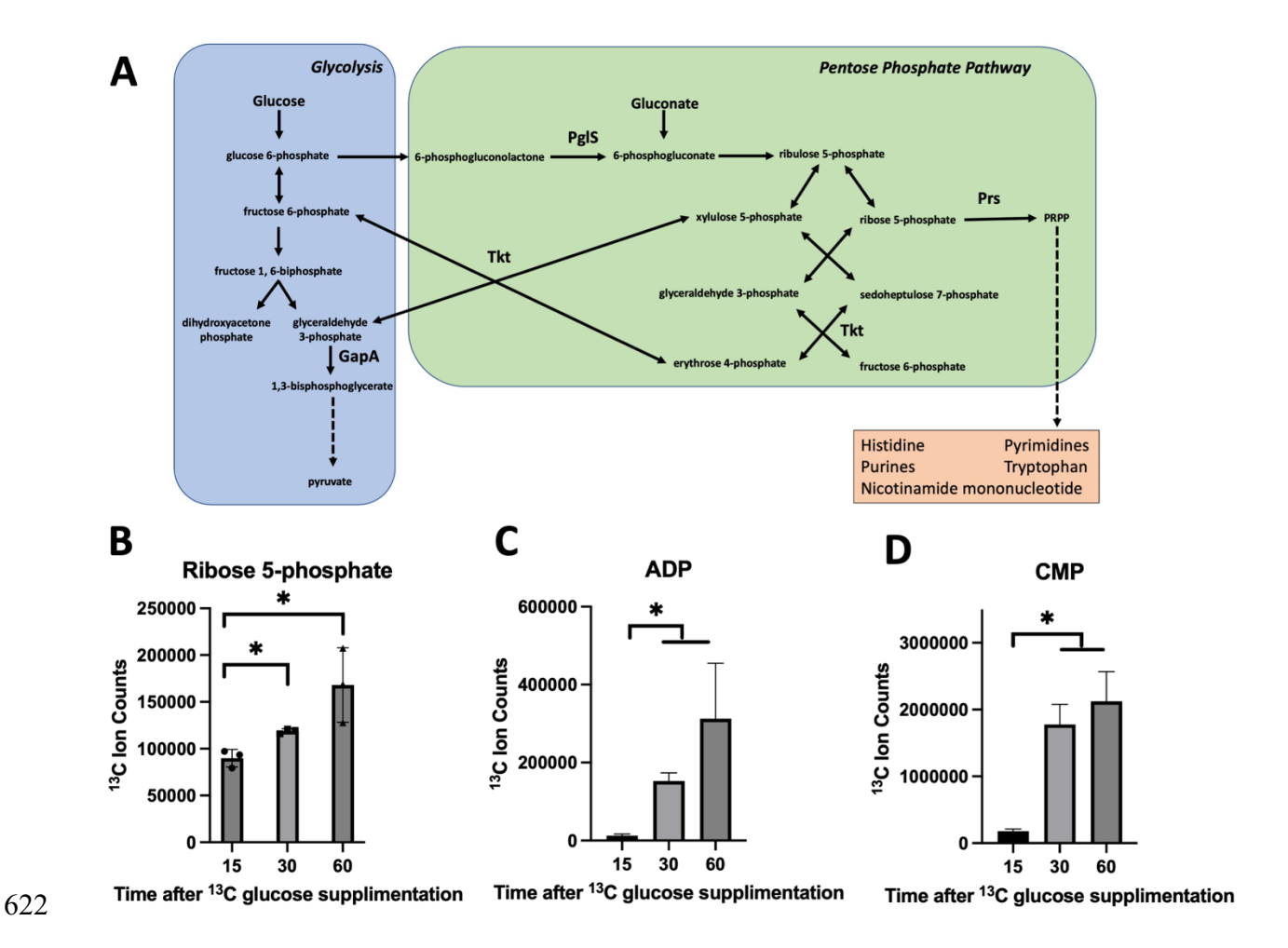
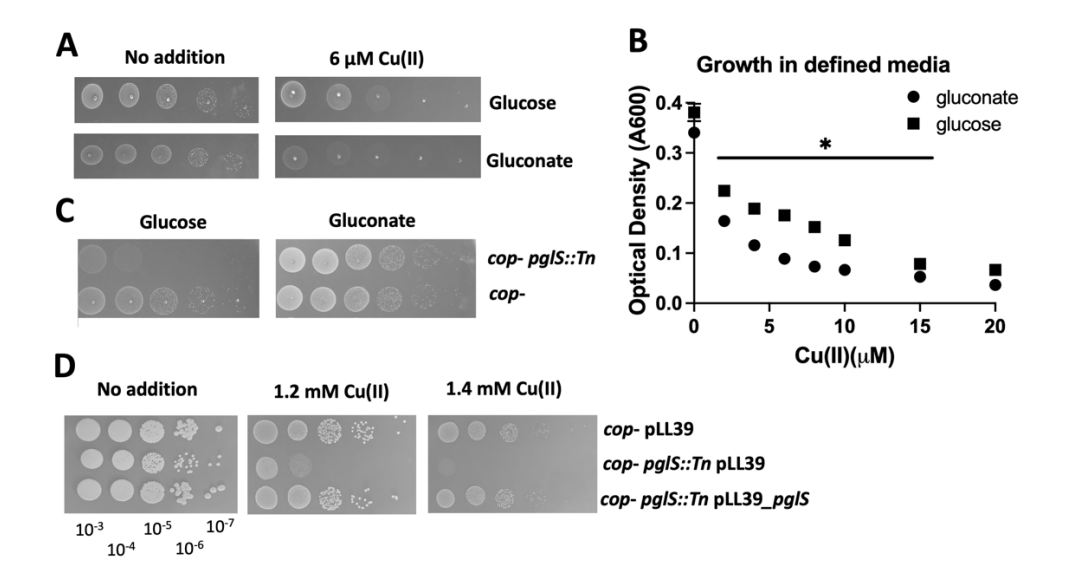


Figure 2. Carbon from glucose is fluxed through the pentose phosphate pathway when growing in TSB medium. Panel A, schematic of the interplay between the glycolytic and pentose phosphate pathways. Key enzymes and metabolites are highlighted. Panels B, C, and D, concentrations of total 13 C carbon atoms in select metabolites after growth in TSB medium containing 13 C glucose. Data represent the average of three biological replicates and standard deviations are displayed. Students t-tests were performed on the data and * indicates p < 0.05.



631

632

633

634

635

636

637

638

639

640

641

642

643

644

Figure 3. Growth with Cu(II) alters pentose phosphate pathway function. Panel A, the copstrain was serial diluted and spot plated on chemically defined media containing either glucose or gluconate as the primary carbon source with and without 6 µM Cu(II). Panel B, the optical densities of cultures of the cop⁻ strain after 18 hours of growth in defined liquid media with 11 mM glucose or gluconate as the primary carbon source and 0-20 μM Cu(II) are presented. The data presented represent the average of three biological replicates and standard deviations are displayed; however, they are too small to be seen for most data points. Students t-tests were performed between culture optical density readings for glucose and gluconate growth at each individual Cu(II) concentration and * indicates p < 0.05. A significant difference in final optical density was noted for all Cu(II) concentrations expect for 0 and 20 µM Cu(II). Panel C, the cop⁻ and cop⁻ pgl::Tn strains were serial diluted and spot plated on defined media containing either 11 mM glucose or gluconate as the primary carbon source. Panel D, the cop⁻ and cop⁻ pgl::Tn strains containing either pLL39 or pLL39 pglS were serial diluted and spot plated on TSA media containing 0 or 1.2 mM Cu(II). Photos of representative experiments displayed.

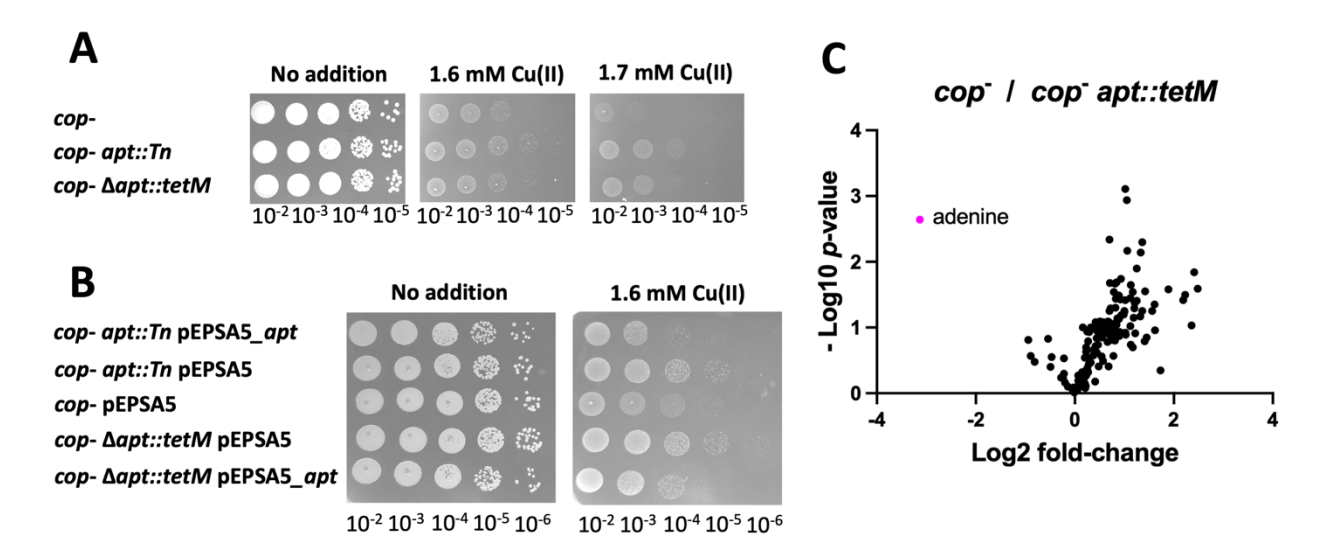


Figure 4. A null mutation in *apt* suppresses the Cu(II) sensitivity of the *cop*⁻ strain. Panel A, overnight cultures of the *cop*⁻, *cop*⁻ *apt::Tn*, and *cop*⁻ Δ*apt::tetM* strains were serially diluted and spot plated on TSA media with 0, 1.6, and 1.7 mM Cu(II). Panel B, overnight cultures of the *cop*⁻, *cop*⁻ *apt::Tn*, and *cop*⁻ Δ*apt::tetM* strains containing the pEPSA5_*apt* or pEPSA5 (empty vector) were serially diluted and spot plated onto TSA chloramphenicol media with 0 or 1.6 mM Cu(II). Panel C, Volcano plots of Log2 fold change of metabolite abundances isolated from *cop*⁻ divided by those of the *cop*⁻ *apt::tetM* strain. Data represent the average of three biological replicates. Photos of representative experiments displayed.

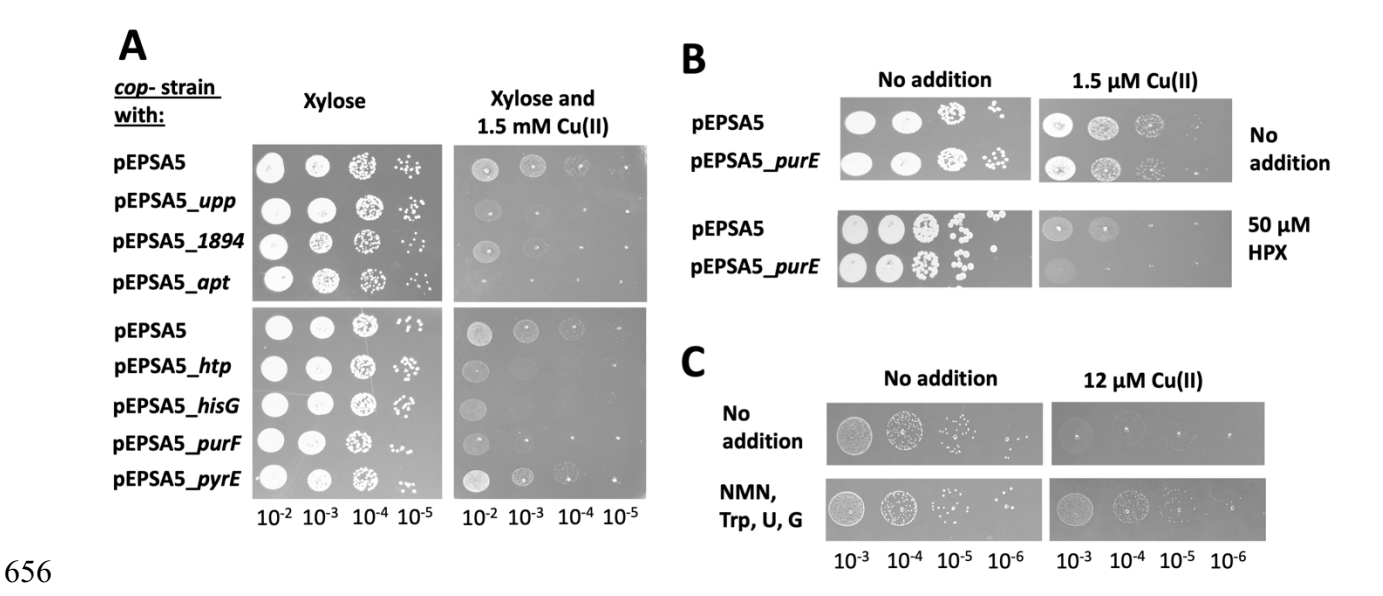


Figure 5. Altering the demand for PRPP modulates the sensitivity to Cu(II). Panel A, cultures of the *cop*⁻ strain containing the empty vector (pEPSA5) or plasmid that over-expresses a gene coding a PRPP utilizing enzyme were serial diluted and spot plated on solid TSA chloramphenicol media containing 0.5% xylose and 0 or 1.5 mM Cu(II). Panel B, cultures of the *cop*⁻ strain containing the empty vector (pEPSA5) or plasmid that over-expresses *purE* were serial diluted and spot plated on solid TSA chloramphenicol media containing 0.5% xylose, 0 or 1.5 mM Cu(II), and with or without 50 μM hypoxanthine (HPX). Panel C, cultures of the *cop*⁻ strain were serial diluted and spot plated on defined glucose medium with 0 or 12 μM Cu(II) and with and without 50 μM uridine (U), tryptophan (Trp), guanosine (G), and nicotinamide mononucleotide (NMN). Photos of representative experiments displayed.

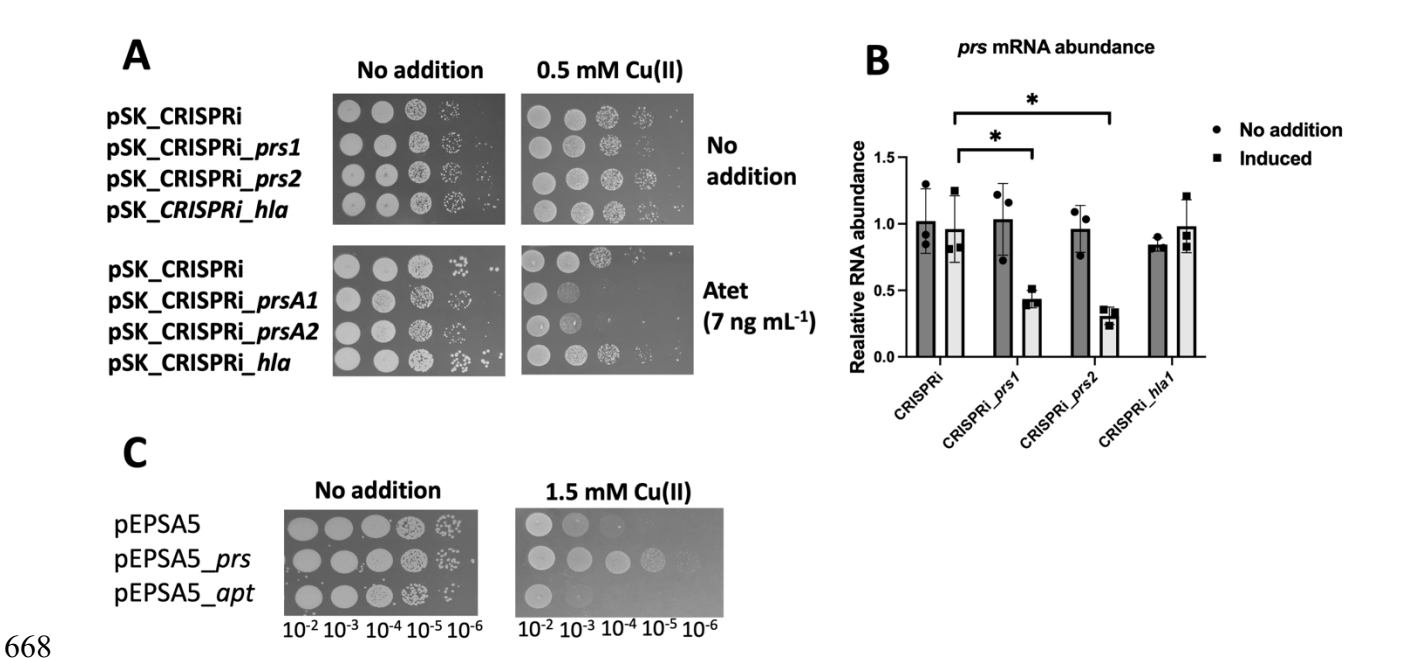


Figure 6. Modulating *prs* expression alters sensitivity to Cu(II). Panel A, cultures of the *cop*⁻ strain containing a pSK_CRIPSRi vector were serial diluted and spot plated on TSA chloramphenicol media with 0 or 0.5 mM Cu(II) with or without 7 ng mL⁻¹ anhydrotetracycline (Atet) to induce *dcas9* expression. The gene targeted by the sgRNA are displayed except for the control which contains a randomized sgRNA (pSK_CRIPSRi). Panel B, the abundances of RNAs corresponding to *prs* were quantified from the same strains listed in Panel A after culture in TSB chloramphenicol media with (dark bars) and without Atet (light bars). Panel C, cultures of the *cop*⁻ strain containing a pESPSA5 (empty vector), pEPSA5_*prs*, or pEPSA5_*apt* were serial diluted and spot plated on TSA chloramphenicol medium with 0 or 1.5 mM Cu(II). The data in Panel B represent the average of three biological replicates and standard deviations are displayed. Students t-tests were performed on the data and * indicates p < 0.05. Photos of representative experiments displayed.

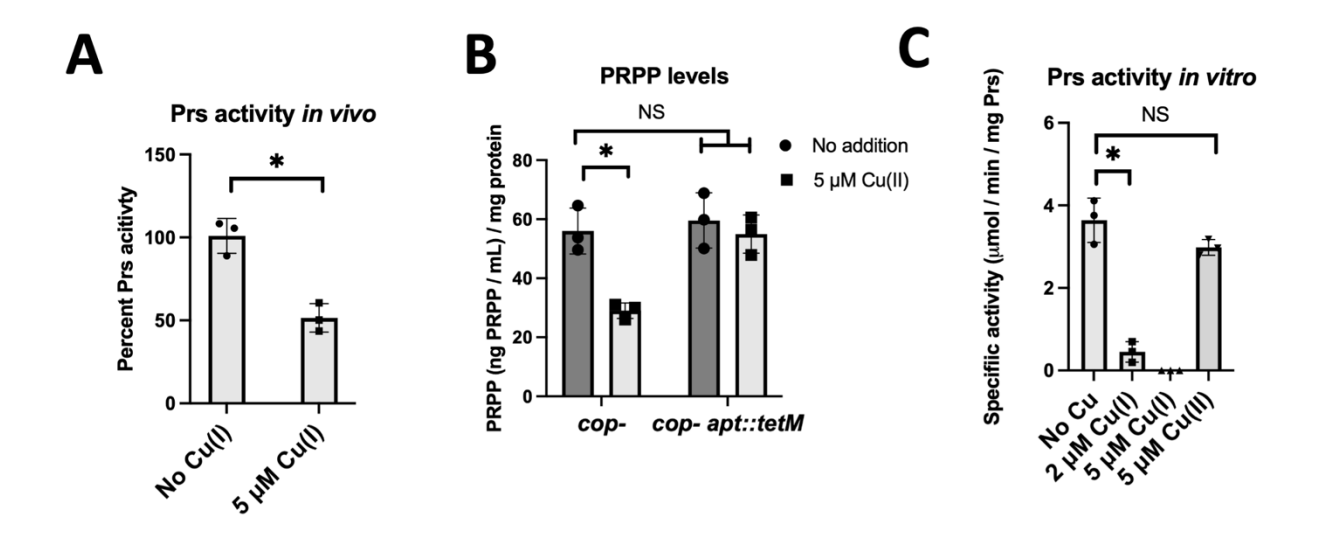


Figure 7. Cu ions inhibit Prs. Panel A, Prs activity was determined in cell-free lysates from the cop^- strain after culture in TSB chloramphenicol medium with 1% xylose and with 0 or 5 μ M Cu(II). Panel B, PRPP levels were determined in cell lysates from the cop^- strain after growth in TSB medium with (dark bars) and without 5 μ M Cu(II) (light bars). Panel C, activity of Prs was monitored in vitro with and without Cu ions. The data displayed are the average of three biological replicates (Panels A and B) or biochemical experiments (Panel C) and standard deviations are displayed. Students t-tests were performed on the data and * indicates p < 0.05.

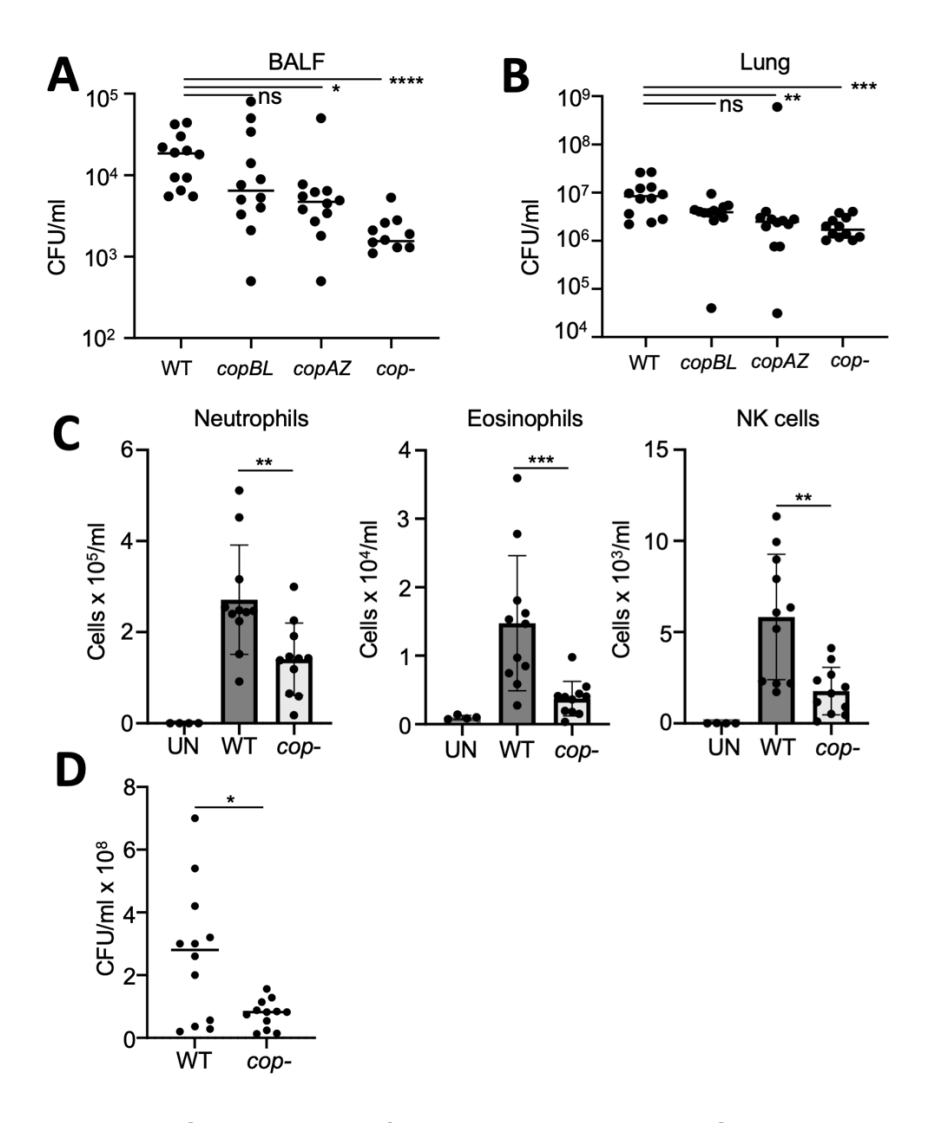


Figure 8. Copper detoxification contributes to *S. aureus* pathogenesis. C57BL/6 mice were intranasally infected with *S. aureus* USA300 and copper transport mutants for 24 h before euthanasia. A) Bacterial counts in BALF. B) Bacterial counts in lung tissue. C) Flow cytometric quantification of recruited immune cells to the airway in BALF. D) C57BL/6 mice were subcutaneously infected with *S. aureus* USA300 and copper transport mutant for five days before euthanasia. Each point represents a mouse. Lines display median. Bar graphs displays means with standard deviation. UN-uninfected, nsnot significant, *P<0.05, **P<0.01, ***P<0.001 and ****P<0.0001.

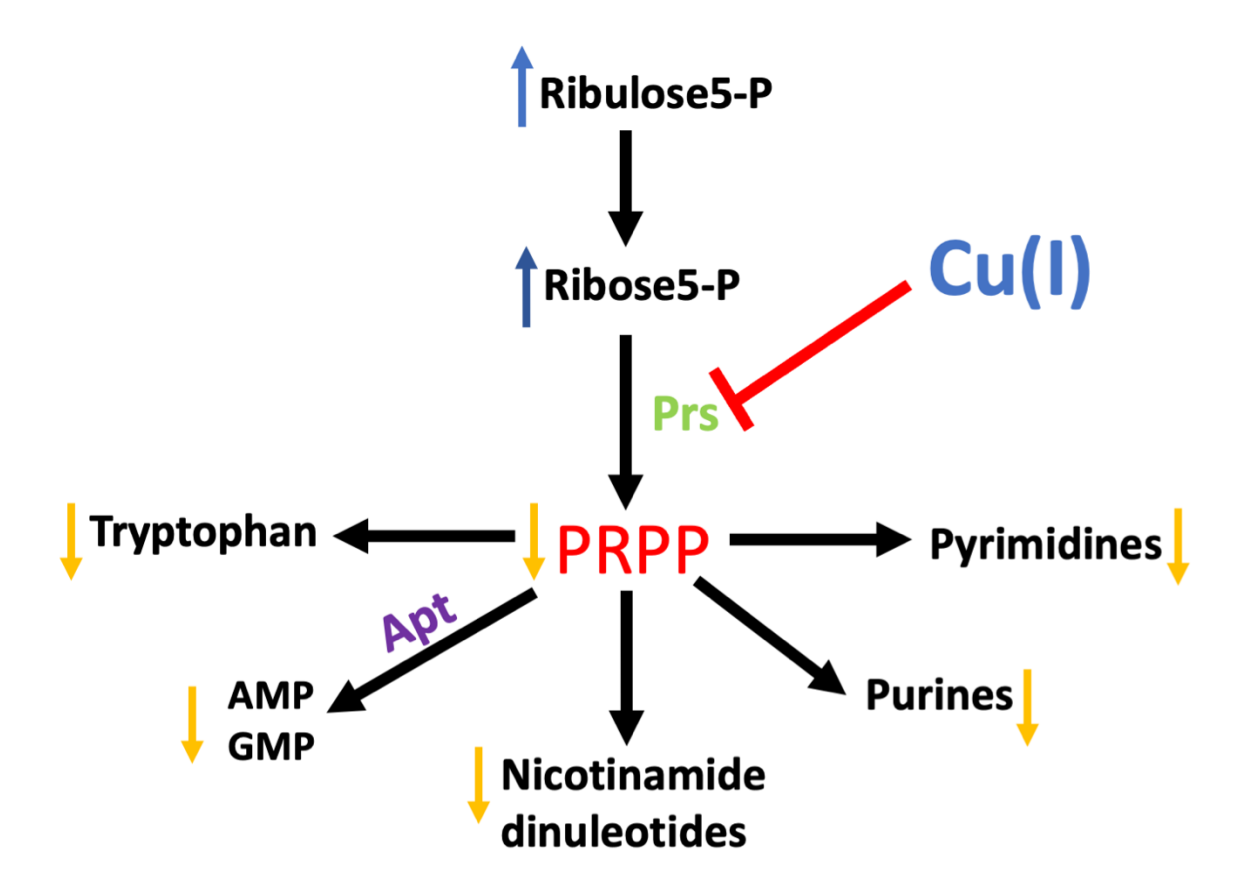


Figure 9. Model for metabolic effects of inhibition of Prs by Cu(I) in *Staphylococcus* aureus.

704 Tables

705

706

707

Table 1. Select metabolites that are significantly altered in the *cop* strain when cultured in presence of 5 μM Cu(II)*

30-minute exposure 60		60-minute exposure		180-minute exposure	
_	Log2 fold-		Log2 fold-		Log2 fold-
metabolite	change	metabolite	change	metabolite	change
Aconitate	1.1	AICA-riboside	0.3	Adenine	1.2
ADP	1.1	Alanine	0.2	Dihydroxyacetone phosphate	2.1
Arginine	1.0	Cystathionine	0.2	3-Phosphoglycerate	2.7
Dihydroxyacetone phosphate	1.1	Glutamine	0.5	Ribose 5-phosphate	0.5
Fructose-1 6-bisphosphate	1.8	Isoleucine	0.4	Serine	-0.5
Fructose-6-phosphate	1.2	Leucine	0.3	Threonine	-0.5
Glucose	1.3	Methionine	0.3		
Glucose 1-phosphate	1.1	Mevalonate	0.3		
Glucose 6-phosphate	1.1	Pantothenate	0.4		
Glycerate	1.2	Ribose 5-phosphate	0.2		
Isocitrate	1.0	Serine	0.6		
Lysine	1.0	Threonine	0.6		
NADH	1.0	Valine	0.3		
NADP	1.1				
Orotate	1.2				
3-Phosphoglycerate	1.7				
Pyruvate	1.1				
Ribitol	1.1				
Ribose 5-phosphate	1.1				
Ribulose-5-phosphate	1.1				
Threonine	1.1				
UDP-Glucose	1.2				
3-Ureidopropionic acid	1.3				

^{*}Experiment was conducted using biological triplicates. All metabolites listed were significantly (students two tailed t-test p < 0.051) altered compared to the untreated sample. A full list of metabolites can be found in Table S1

Table 2. Select metabolites containing significant quantities of ¹³C after growth with ¹³C glucose*

Glycolysis	<u>Purines</u>	<u>Pyrimidines</u>
glucose 6-phosphate	GMP	CMP
3-phosphoglycerate	dGMP	UMP
glycerol 3-phosphate	AMP	dUMP
phosphoenolpyruvate	dAMP	dTMP
pyruvate	AMP	uracil
	AICAR	
Pentose phosphate pathway	AICA-riboside	
Ribose 5-phosphate		Nicotinamide cofactors
sedoheptulose 7-phosphate		NAD ⁺
Ribose		NADH

^{*}a full list of metabolites can be found in Table S2.

712

Table 3. Significantly altered metabolites in the *cop*⁻ Δ*apt::tetM* strain.^a*

cop⁻ / cop⁻ ∆apt			
Metabolite	Log2 fold-change		
Adenine	-3.1		
AICAR (ZMP)	2.2		
AICA-riboside	0.8		
Cytosine	1.0		
dÜMP	1.9		
Lactate	1.2		
Mevalonate	2.2		
Orotate ^b	>10		
Ribose 5-phosphate	1.6		
Sedoheptulose	2.4		
UDP-Glucose	0.9		

^a A paired student t-test was run and metabolites with a p <0.05 displayed.

^b Orotate was below the detectable limit upon

Cu addition.

^{*} A full list of metabolites can be found in Table S3.

Table 4. S. aureus PRPP utilizing enzymes.

Enzyme	Reaction	Name	Locus tag
Ribose-phosphate pyrophosphokinase	AMP + PRPP = ribose 5-phosphate + ATP	Prs	SAUSA300_0478
Nicotinate phosphoribosyltransferase	nicotinate + PRPP + ATP = β -nicotinate D-ribonucleotide + PP _i + ADP + P _i		SAUSA300_1894
Adenine phosphoribosyltransferase	PRPP + adenine = AMP + PP _i	Apt	SAUSA300_1591
ATP phosphoribosyltransferase	PRPP +ATP = 1-(5-phospho-β-D-ribosyl)- ATP + diphosphate	HisG	SAUSA300_2612
Hypoxanthine-guanine phosphoribosyltransferase	hypoxanthine + PRPP = inosine monophosphate	Hpt	SAUSA300_0488
	guanine + PRPP = guanosine monophosphate.		
Uracil phosphoribosyltransferase	Uracil + PRPP = UMP	Upp	SAUSA300_2066
Anthranilate phosphoribosyltransferase	Anthranilate + PRPP = N-(5-phospho-D-ribosyl)-anthranilate + PP _i	TrpD	SAUSA300_1264
Orotate phosphoribosyltransferase	Orotate + PRPP = orotidine 5'-phosphate + PP _i	PyrE	SAUSA300_1098
Amidophosphoribosyltransferase	PRPP + H ₂ O + glutamine = 5-phospho-β-D- ribosylamine + diphosphate + glutamate	PurF	SAUSA300_0972
Xanthine phosphoribosyltransferase	XMP + diphosphate = 5-phospho-alpha-D-ribose 1-diphosphate + xanthine	Xpt	SAUSA300_0386

Table 5. Strains and plasmids used in this study.

Microbial	etraine	hazilitu	in	thie	etudy
WIICI ODIAI	วแลแเ ว	uuuzeu	111	นเมอ	Stuuv

Name	Chromosomal Genotype ^a	Reference
S. aureus USA300 LAC strains		
JMB 8573	$\triangle copBL \ \triangle copAZ \ (cop^{-})$	[31]
JMB 7901	$\Delta copBL$	[5]
JMB 8571	$\Delta copAZ$	[31]
JMB 8902	cop ⁻ apt::Tn (ermB) (SAUSA300_1591)	[31]
JMB 9138	cop⁻ ∆apt::tetR (SAUSA300_1591)	This study
JMB 10462	cop ⁻ pglS::Tn(ermB)(SAUSA300_1902)	This study and [76]
JMB 11379	cop⁻ ∆tkt::kan (SAUSA300_1239)	This study and [77]
JMB 9535	cop ⁻ pLL39	[32]
JMB 13670	cop ⁻ pglS::Tn pLL39	This study and
JMB 13672	cop ⁻ pglS::Tn pLL39_pglS	This study and
Other strains		
RN4220	Restriction minus S. aureus	[67]
DH5α	Restriction minus E. coli	
BL21 AI*	Expression E. coli	
FY2	S. cerevisiae for YCC	[78]

Plasmids used in this study

Name	Function	Reference
pJB38	Construction of gene deletions	[79]
pEPSA5	XyIR dependent transcription	[80]
pSK	Shuttle vector	[81]
pSK_CRISPR	Expression of CRISPR/dCas9 system	[43] and this study
pSK_CRISPR_ <i>hla</i>	CRISPR/dCas9 directed at hla	[43] and this study
pSK_CRISPR_ <i>prsA1</i>	CRISPR/dCas9 directed at prsA	This study
pSK_CRISPR_prsA2	CRISPR/dCas9 directed at prsA	This study
pEPSA5 <i>_apt</i>	apt under xylose inducible promoter	This study
pLL39	Genetic complementation	[82]
pLL39_pglS	pglS under native promoter	This study
pEPSA5_ <i>prsA</i>	prsA under xylose inducible promoter	This study
pEPSA5 hpt	hpt under xylose inducible promoter	This study
pEPSA5 hisG	hisG under xylose inducible promoter	This study
pEPSA5_ <i>purF</i>	purF under xylose inducible promoter	This study
pEPSA5_ <i>pyrE</i>	pyrF under xylose inducible promoter	This study
pEPSA5 <i>_1894</i>	1894 under xylose inducible promoter	This study
pGEX-6P-1 <i>_prsA</i>	Expression of Prs for purification	This study
pJB38_Δ <i>apt::tetM</i>	Generate ∆apt::tetM allele	This study
^a Abbreviations: <i>Tn</i> , transp	oson	

Supplemental information for Copper ions inhibit pentose phosphate pathway function in Staphylococcus aureus. Javiera Norambuena, Hassan Al-Tameemi, Hannah Bovermann, Jisun Kim, William N. Beavers, Eric P. Skaar, Dane Parker, Jeffrey M. Boyd* *To whom correspondence may be addressed: Jeffrey M. Boyd, Department of Biochemistry and Microbiology, Rutgers University, 76 Lipman Drive, New Brunswick, New Jersey, 08901, Telephone: (848) 932-5604, E-mail: jeffboyd@SEBS.rutgers.edu.

References

- 1. Elguindi J, Wagner J, Rensing C. Genes involved in copper resistance influence survival of
- 734 Pseudomonas aeruginosa on copper surfaces. J Appl Microbiol. 2009;106(5):1448-55. Epub 20090223.
- 735 doi: 10.1111/j.1365-2672.2009.04148.x. PubMed PMID: 19239551; PubMed Central PMCID:
- 736 PMCPMC3991433.
- 2. Espirito Santo C, Taudte N, Nies DH, Grass G. Contribution of copper ion resistance to survival of
- 738 Escherichia coli on metallic copper surfaces. Appl Environ Microbiol. 2008;74(4):977-86. Epub 20071221.
- doi: 10.1128/AEM.01938-07. PubMed PMID: 18156321; PubMed Central PMCID: PMCPMC2258564.
- 740 3. Molteni C, Abicht HK, Solioz M. Killing of bacteria by copper surfaces involves dissolved copper.
- 741 Appl Environ Microbiol. 2010;76(12):4099-101. Epub 20100423. doi: 10.1128/AEM.00424-10. PubMed
- 742 PMID: 20418419; PubMed Central PMCID: PMCPMC2893463.
- 4. Espirito Santo C, Lam EW, Elowsky CG, Quaranta D, Domaille DW, Chang CJ, et al. Bacterial killing
- by dry metallic copper surfaces. Appl Environ Microbiol. 2011;77(3):794-802. Epub 20101210. doi:
- 745 10.1128/AEM.01599-10. PubMed PMID: 21148701; PubMed Central PMCID: PMCPMC3028699.
- 746 5. Rosario-Cruz Z, Eletsky A, Daigham NS, Al-Tameemi H, Swapna GVT, Kahn PC, et al. The copBL
- operon protects Staphylococcus aureus from copper toxicity: CopL is an extracellular membrane-
- 748 associated copper-binding protein. J Biol Chem. 2019;294(11):4027-44. Epub 2019/01/19. doi:
- 749 10.1074/jbc.RA118.004723. PubMed PMID: 30655293.
- 750 6. Macomber L, Imlay JA. The iron-sulfur clusters of dehydratases are primary intracellular targets
- 751 of copper toxicity. Proc Natl Acad Sci U S A. 2009;106(20):8344-9. PubMed PMID: 19416816.
- 752 7. Djoko KY, McEwan AG. Antimicrobial action of copper is amplified via inhibition of heme
- 753 biosynthesis. ACS Chem Biol. 2013;8(10):2217-23. Epub 2013/07/31. doi: 10.1021/cb4002443. PubMed PMID: 23895035.
- 755 8. Imlay JA. Cellular defenses against superoxide and hydrogen peroxide. Annu Rev Biochem.
- 756 2008;77:755-76. PubMed PMID: 18173371.
- 757 9. Tan G, Yang J, Li T, Zhao J, Sun S, Li X, et al. Anaerobic Copper Toxicity and Iron-Sulfur Cluster
- 758 Biogenesis in Escherichia coli. Appl Environ Microbiol. 2017;83(16). Epub 2017/06/04. doi:
- 759 10.1128/AEM.00867-17. PubMed PMID: 28576762; PubMed Central PMCID: PMCPMC5541227.
- 760 10. Chillappagari S, Seubert A, Trip H, Kuipers OP, Marahiel MA, Miethke M. Copper stress affects
- 761 iron homeostasis by destabilizing iron-sulfur cluster formation in *Bacillus subtilis*. J Bacteriol.
- 762 2010;192(10):2512-24. PubMed PMID: 20233928.
- Tan G, Cheng Z, Pang Y, Landry AP, Li J, Lu J, et al. Copper binding in IscA inhibits iron-sulphur
- 764 cluster assembly in *Escherichia coli*. Mol Microbiol. 2014;93(4):629-44. doi: 10.1111/mmi.12676.
- PubMed PMID: 24946160; PubMed Central PMCID: PMCPMC4132641.
- 766 12. Brancaccio D, Gallo A, Piccioli M, Novellino E, Ciofi-Baffoni S, Banci L. [4Fe-4S] Cluster Assembly
- in Mitochondria and Its Impairment by Copper. J Am Chem Soc. 2017;139(2):719-30. Epub 2016/12/19.
- 768 doi: 10.1021/jacs.6b09567. PubMed PMID: 27989128.
- 13. Imlay JA, Chin SM, Linn S. Toxic DNA Damage by Hydrogen Peroxide through the Fenton
- 770 Reaction in vivo and in vitro. Science. 1988;240(4852):640-2.
- 771 14. Wink DA, Wink CB, Nims RW, Ford PC. Oxidizing intermediates generated in the Fenton reagent:
- kinetic arguments against the intermediacy of the hydroxyl radical. Environmental Health Perspectives.
- 773 1994;102(Suppl 3):11-5. PubMed PMID: PMC1567375.
- 774 15. Macomber L, Rensing C, Imlay JA. Intracellular copper does not catalyze the formation of
- 775 oxidative DNA damage in *Escherichia coli*. J Bacteriol. 2007;189(5):1616-26. Epub 2006/12/26. doi:
- 776 10.1128/JB.01357-06. PubMed PMID: 17189367; PubMed Central PMCID: PMCPMC1855699.

- 16. Hodgkinson V, Petris MJ. Copper homeostasis at the host-pathogen interface. J Biol Chem.
- 778 2012;287(17):13549-55. Epub 2012/03/06. doi: 10.1074/jbc.R111.316406. PubMed PMID: 22389498;
- 779 PubMed Central PMCID: PMCPMC3340201.
- 780 17. Beveridge SJ, Garrett IR, Whitehouse MW, Vernon-Roberts B, Brooks PM. Biodistribution of ⁶⁴Cu
- in inflamed rats following administration of two anti-inflammatory copper complexes. Agents Actions.
- 782 1985;17(1):104-11. Epub 1985/10/01. PubMed PMID: 3878667.
- 783 18. Focarelli F, Giachino A, Waldron KJ. Copper microenvironments in the human body define
- patterns of copper adaptation in pathogenic bacteria. PLoS Pathog. 2022;18(7):e1010617. Epub
- 785 20220721. doi: 10.1371/journal.ppat.1010617. PubMed PMID: 35862345; PubMed Central PMCID:
- 786 PMCPMC9302775.
- 787 19. Achard ME, Stafford SL, Bokil NJ, Chartres J, Bernhardt PV, Schembri MA, et al. Copper
- redistribution in murine macrophages in response to *Salmonella* infection. Biochem J. 2012;444(1):51-7.
- 789 Epub 2012/03/01. doi: 10.1042/BJ20112180. PubMed PMID: 22369063.
- 790 20. Wagner D, Maser J, Lai B, Cai Z, Barry CE, 3rd, Honer Zu Bentrup K, et al. Elemental analysis of
- 791 Mycobacterium avium-, Mycobacterium tuberculosis-, and Mycobacterium smegmatis-containing
- 792 phagosomes indicates pathogen-induced microenvironments within the host cell's endosomal system. J
- 793 Immunol. 2005;174(3):1491-500. Epub 2005/01/22. PubMed PMID: 15661908.
- 794 21. White C, Lee J, Kambe T, Fritsche K, Petris MJ. A role for the ATP7A copper-transporting ATPase
- 795 in macrophage bactericidal activity. J Biol Chem. 2009;284(49):33949-56. Epub 2009/10/08. doi:
- 796 10.1074/jbc.M109.070201. PubMed PMID: 19808669; PubMed Central PMCID: PMCPMC2797165.
- 797 22. Zapotoczna M, Riboldi GP, Moustafa AM, Dickson E, Narechania A, Morrissey JA, et al. Mobile-
- 798 Genetic-Element-Encoded Hypertolerance to Copper Protects Staphylococcus aureus from Killing by
- 799 Host Phagocytes. mBio. 2018;9(5). Epub 2018/10/18. doi: 10.1128/mBio.00550-18. PubMed PMID:
- 800 30327441; PubMed Central PMCID: PMCPMC6191537.
- 801 23. Purves J, Thomas J, Riboldi GP, Zapotoczna M, Tarrant E, Andrew PW, et al. A horizontally gene
- transferred copper resistance locus confers hyper-resistance to antibacterial copper toxicity and enables
- survival of community acquired methicillin resistant *Staphylococcus aureus* USA300 in macrophages.
- 804 Environmental microbiology. 2018;20(4):1576-89. Epub 2018/03/10. doi: 10.1111/1462-2920.14088.
- PubMed PMID: 29521441; PubMed Central PMCID: PMCPMC5947656.
- 806 24. Saenkham-Huntsinger P, Hyre AN, Hanson BS, Donati GL, Adams LG, Ryan C, et al. Copper
- 807 Resistance Promotes Fitness of Methicillin-Resistant Staphylococcus aureus during Urinary Tract
- 808 Infection. mBio. 2021;12(5):e0203821. Epub 20210907. doi: 10.1128/mBio.02038-21. PubMed PMID:
- 809 34488457; PubMed Central PMCID: PMCPMC8546587.
- 810 25. Arguello JM, Eren E, Gonzalez-Guerrero M. The structure and function of heavy metal transport
- 811 P1B-ATPases. Biometals. 2007;20(3-4):233-48. Epub 2007/01/16. doi: 10.1007/s10534-006-9055-6.
- 812 PubMed PMID: 17219055.
- 813 26. Singleton C, Hearnshaw S, Zhou L, Le Brun NE, Hemmings AM. Mechanistic insights into Cu(I)
- cluster transfer between the chaperone CopZ and its cognate Cu(I)-transporting P-type ATPase, CopA.
- 815 Biochem J. 2009;424(3):347-56. Epub 2009/09/16. doi: 10.1042/BJ20091079. PubMed PMID: 19751213.
- 816 27. Planet PJ, Diaz L, Kolokotronis SO, Narechania A, Reyes J, Xing G, et al. Parallel Epidemics of
- 817 Community-Associated Methicillin-Resistant Staphylococcus aureus USA300 Infection in North and
- 818 South America. J Infect Dis. 2015;212(12):1874-82. doi: 10.1093/infdis/jiv320. PubMed PMID: 26048971;
- PubMed Central PMCID: PMCPMC4655856.
- 820 28. Moore CM, Gaballa A, Hui M, Ye RW, Helmann JD. Genetic and physiological responses of
- 821 Bacillus subtilis to metal ion stress. Mol Microbiol. 2005;57(1):27-40. Epub 2005/06/14. doi:
- 822 10.1111/j.1365-2958.2005.04642.x. PubMed PMID: 15948947.
- 823 29. Baker J, Sitthisak S, Sengupta M, Johnson M, Jayaswal RK, Morrissey JA. Copper stress induces a
- 824 global stress response in Staphylococcus aureus and represses sae and agr expression and biofilm

- 825 formation. Appl Environ Microbiol. 2010;76(1):150-60. doi: 10.1128/AEM.02268-09. PubMed PMID:
- 826 19880638; PubMed Central PMCID: PMCPMC2798663.
- 827 30. Quintana J, Novoa-Aponte L, Arguello JM. Copper homeostasis networks in the bacterium
- 828 Pseudomonas aeruginosa. J Biol Chem. 2017;292(38):15691-704. Epub 2017/08/02. doi:
- 829 10.1074/jbc.M117.804492. PubMed PMID: 28760827; PubMed Central PMCID: PMCPMC5612103.
- 830 31. Al-Tameemi H, Beavers WN, Norambuena J, Skaar EP, Boyd JM. Staphylococcus aureus lacking a
- functional MntABC manganese import system has increased resistance to copper. Mol Microbiol.
- 832 2021;115(4):554-73. Epub 2020/10/10. doi: 10.1111/mmi.14623. PubMed PMID: 33034093; PubMed
- 833 Central PMCID: PMCPMC8121185.
- 834 32. Al-Tameemi H, Beavers WN, Norambuena J, Skaar EP, Boyd JM. Staphylococcus aureus lacking a
- functional MntABC manganese import system has increased resistance to copper. Mol Microbiol. 2020.
- 836 Epub 2020/10/10. doi: 10.1111/mmi.14623. PubMed PMID: 33034093.
- 33. Tarrant E, P Riboldi G, McIlvin MR, Stevenson J, Barwinska-Sendra A, Stewart LJ, et al. Copper
- 838 stress in Staphylococcus aureus leads to adaptive changes in central carbon metabolism. Metallomics :
- integrated biometal science. 2019;11(1):183-200. doi: 10.1039/c8mt00239h. PubMed PMID: 30443649.
- 840 34. Kupor SR, Fraenkel DG. Glucose metabolism in 6 phosphogluconolactonase mutants of
- 841 Escherichia coli. J Biol Chem. 1972;247(6):1904-10. PubMed PMID: 4552019.
- 842 35. Hochstadt-Ozer J, Stadtman ER. The Regulation of Purine Utilization in Bacteria: I. PURIFICATION
- 843 OF ADENINE PHOSPHORIBOSYLTRANSFERASE FROM ESCHERICHIA COLI K12 AND CONTROL OF ACTIVITY
- 844 BY NUCLEOTIDES. Journal of Biological Chemistry. 1971;246(17):5294-303. doi:
- 845 https://doi.org/10.1016/S0021-9258(18)61906-4.
- 846 36. Hove-Jensen B, Andersen KR, Kilstrup M, Martinussen J, Switzer RL, Willemoës M.
- Phosphoribosyl Diphosphate (PRPP): Biosynthesis, Enzymology, Utilization, and Metabolic Significance.
- 848 Microbiol Mol Biol Rev. 2016;81(1):e00040-16. doi: 10.1128/MMBR.00040-16. PubMed PMID:
- 849 28031352.
- 850 37. Nygaard P, Saxild HH. Nucleotide Metabolism. In: Schaechter M, editor. Encyclopedia of
- Microbiology (Third Edition). Oxford: Academic Press; 2009. p. 296-307.
- 852 38. Hochstadt J. Hypoxanthine phosphoribosyltransferase and guanine phosphoribosyltransferase
- from enteric bacteria. Methods in enzymology. 51: Academic Press; 1978. p. 549-58.
- 854 39. Hove-Jensen B. Mutation in the phosphoribosylpyrophosphate synthetase gene (prs) that results
- in simultaneous requirements for purine and pyrimidine nucleosides, nicotinamide nucleotide, histidine,
- and tryptophan in *Escherichia coli*. J Bacteriol. 1988;170(3):1148-52. doi: 10.1128/jb.170.3.1148-
- 857 1152.1988. PubMed PMID: 2449419; PubMed Central PMCID: PMCPMC210885.
- 858 40. Flensburg J, Skold O. Massive overproduction of dihydrofolate reductase in bacteria as a
- 859 response to the use of trimethoprim. Eur J Biochem. 1987;162(3):473-6. doi: 10.1111/j.1432-
- 860 1033.1987.tb10664.x. PubMed PMID: 3549289.
- 861 41. Peters JM, Koo BM, Patino R, Heussler GE, Hearne CC, Qu J, et al. Enabling genetic analysis of
- diverse bacteria with Mobile-CRISPRi. Nat Microbiol. 2019;4(2):244-50. Epub 20190107. doi:
- 863 10.1038/s41564-018-0327-z. PubMed PMID: 30617347; PubMed Central PMCID: PMCPMC6424567.
- 42. Qi LS, Larson MH, Gilbert LA, Doudna JA, Weissman JS, Arkin AP, et al. Repurposing CRISPR as an
- RNA-guided platform for sequence-specific control of gene expression. Cell. 2013;152(5):1173-83. doi:
- 866 10.1016/j.cell.2013.02.022. PubMed PMID: 23452860; PubMed Central PMCID: PMCPMC3664290.
- 43. Zhao C, Shu X, Sun B. Construction of a Gene Knockdown System Based on Catalytically Inactive
- 868 ("Dead") Cas9 (dCas9) in Staphylococcus aureus. Appl Environ Microbiol. 2017;83(12). Epub 20170531.
- doi: 10.1128/AEM.00291-17. PubMed PMID: 28411216; PubMed Central PMCID: PMCPMC5452804.
- 870 44. Todd OA, Fidel PL, Jr., Harro JM, Hilliard JJ, Tkaczyk C, Sellman BR, et al. Candida albicans
- 871 Augments Staphylococcus aureus Virulence by Engaging the Staphylococcal agr Quorum Sensing System.

- 872 mBio. 2019;10(3). Epub 20190604. doi: 10.1128/mBio.00910-19. PubMed PMID: 31164467; PubMed
- 873 Central PMCID: PMCPMC6550526.
- 45. Grosser MR, Paluscio E, Thurlow LR, Dillon MM, Cooper VS, Kawula TH, et al. Genetic
- requirements for *Staphylococcus aureus* nitric oxide resistance and virulence. PLoS Pathog.
- 876 2018;14(3):e1006907. Epub 2018/03/20. doi: 10.1371/journal.ppat.1006907. PubMed PMID: 29554137;
- PubMed Central PMCID: PMCPMC5884563.
- 878 46. Koenigsknecht MJ, Fenlon LA, Downs DM. Phosphoribosylpyrophosphate synthetase (PrsA)
- variants alter cellular pools of ribose 5-phosphate and influence thiamine synthesis in Salmonella
- enterica. Microbiology (Reading). 2010;156(Pt 3):950-9. Epub 2009/12/03. doi: 10.1099/mic.0.033050-0.
- 881 PubMed PMID: 19959576.
- 47. Carrasco-Pozo C, Aliaga ME, Olea-Azar C, Speisky H. Double edge redox-implications for the
- interaction between endogenous thiols and copper ions: *In vitro* studies. Bioorg Med Chem.
- 884 2008;16(22):9795-803. Epub 20081001. doi: 10.1016/j.bmc.2008.09.068. PubMed PMID: 18926709.
- 48. Yajjala VK, Thomas VC, Bauer C, Scherr TD, Fischer KJ, Fey PD, et al. Resistance to Acute
- 886 Macrophage Killing Promotes Airway Fitness of Prevalent Community-Acquired Staphylococcus aureus
- Strains. J Immunol. 2016;196(10):4196-203. Epub 20160406. doi: 10.4049/jimmunol.1600081. PubMed
- 888 PMID: 27053759; PubMed Central PMCID: PMCPMC4868659.
- 889 49. Pidwill GR, Gibson JF, Cole J, Renshaw SA, Foster SJ. The Role of Macrophages in *Staphylococcus*
- 890 *aureus* Infection. Front Immunol. 2020;11:620339. Epub 20210119. doi: 10.3389/fimmu.2020.620339.
- PubMed PMID: 33542723; PubMed Central PMCID: PMCPMC7850989.
- 892 50. Rohaun SK, Imlay JA. The vulnerability of radical SAM enzymes to oxidants and soft metals.
- 893 Redox Biol. 2022;57:102495. Epub 20221007. doi: 10.1016/j.redox.2022.102495. PubMed PMID:
- 894 36240621; PubMed Central PMCID: PMCPMC9576991.
- 895 51. Esquilin-Lebron K, Dubrac S, Barras F, Boyd JM. Bacterial Approaches for Assembling Iron-Sulfur
- 896 Proteins. mBio. 2021;12(6):e0242521. Epub 20211116. doi: 10.1128/mBio.02425-21. PubMed PMID:
- 897 34781750; PubMed Central PMCID: PMCPMC8593673.
- 898 52. Vinella D, Brochier-Armanet C, Loiseau L, Talla E, Barras F. Iron-sulfur (Fe/S) protein biogenesis:
- phylogenomic and genetic studies of A-type carriers. PLoS Genet. 2009;5(5):e1000497. PubMed PMID:
- 900 19478995.
- 901 53. Roberts CA, Al-Tameemi HM, Mashruwala AA, Rosario-Cruz Z, Chauhan U, Sause WE, et al. The
- 902 Suf Iron-Sulfur Cluster Biosynthetic System Is Essential in Staphylococcus aureus, and Decreased Suf
- 903 Function Results in Global Metabolic Defects and Reduced Survival in Human Neutrophils. Infect Immun.
- 904 2017;85(6). Epub 2017/03/23. doi: 10.1128/IAI.00100-17. PubMed PMID: 28320837; PubMed Central
- 905 PMCID: PMCPMC5442634.
- 906 54. Mashruwala AA, Bhatt S, Poudel S, Boyd ES, Boyd JM. The DUF59 Containing Protein SufT Is
- 907 Involved in the Maturation of Iron-Sulfur (FeS) Proteins during Conditions of High FeS Cofactor Demand
- 908 in Staphylococcus aureus. PLoS Genet. 2016;12(8):e1006233. doi: 10.1371/journal.pgen.1006233.
- 909 PubMed PMID: 27517714.
- 910 55. Mashruwala AA, Van De Guchte A, Boyd JM. Impaired respiration elicits SrrAB-dependent
- 911 programmed cell lysis and biofilm formation in *Staphylococcus aureus*. eLife. 2017;6. doi:
- 912 10.7554/eLife.23845. PubMed PMID: 28221135.
- 56. Zuily L, Lahrach N, Fassler R, Genest O, Faller P, Seneque O, et al. Copper Induces Protein
- Aggregation, a Toxic Process Compensated by Molecular Chaperones. mBio. 2022;13(2):e0325121. Epub
- 915 20220315. doi: 10.1128/mbio.03251-21. PubMed PMID: 35289645; PubMed Central PMCID:
- 916 PMCPMC9040851.
- 917 57. Farrell RE, Germida JJ, Huang PM. Effects of chemical speciation in growth media on the toxicity
- 918 of mercury(II). Appl Environ Microbiol. 1993;59(5):1507-14. doi: 10.1128/aem.59.5.1507-1514.1993.
- 919 PubMed PMID: 8517745; PubMed Central PMCID: PMCPMC182111.

- 920 58. Switzer RL. Regulation and mechanism of phosphoribosylpyrophosphate synthetase. 3. Kinetic
- studies of the reaction mechanism. J Biol Chem. 1971;246(8):2447-58. PubMed PMID: 4324215.
- 922 59. Zhou W, Tsai A, Dattmore DA, Stives DP, Chitrakar I, D'Alessandro A M, et al. Crystal structure of
- 923 E. coli PRPP synthetase. BMC Struct Biol. 2019;19(1):1. Epub 20190115. doi: 10.1186/s12900-019-0100-
- 4. PubMed PMID: 30646888; PubMed Central PMCID: PMCPMC6332680.
- 925 60. Eriksen TA, Kadziola A, Bentsen AK, Harlow KW, Larsen S. Structural basis for the function of
- 926 Bacillus subtilis phosphoribosyl-pyrophosphate synthetase. Nat Struct Biol. 2000;7(4):303-8. doi:
- 927 10.1038/74069. PubMed PMID: 10742175.
- 928 61. Tarrant E, G PR, McIlvin MR, Stevenson J, Barwinska-Sendra A, Stewart LJ, et al. Copper stress in
- 929 Staphylococcus aureus leads to adaptive changes in central carbon metabolism. Metallomics: integrated
- 930 biometal science. 2019;11(1):183-200. Epub 2018/11/18. doi: 10.1039/c8mt00239h. PubMed PMID:
- 931 30443649; PubMed Central PMCID: PMCPMC6350627.
- Baker J, Sengupta M, Jayaswal RK, Morrissey JA. The *Staphylococcus aureus* CsoR regulates both
- 933 chromosomal and plasmid-encoded copper resistance mechanisms. Environmental microbiology.
- 934 2011;13(9):2495-507. doi: 10.1111/j.1462-2920.2011.02522.x. PubMed PMID: 21812885.
- 935 63. Grossoehme N, Kehl-Fie TE, Ma Z, Adams KW, Cowart DM, Scott RA, et al. Control of copper
- 936 resistance and inorganic sulfur metabolism by paralogous regulators in Staphylococcus aureus. J Biol
- 937 Chem. 2011;286(15):13522-31. Epub 2011/02/23. doi: 10.1074/jbc.M111.220012. PubMed PMID:
- 938 21339296; PubMed Central PMCID: PMCPMC3075698.
- 939 64. Krotkiewska B, Banas T. Interaction of Zn2+ and Cu2+ ions with glyceraldehyde-3-phosphate
- 940 dehydrogenase from bovine heart and rabbit muscle. Int J Biochem. 1992;24(9):1501-5. doi:
- 941 10.1016/0020-711x(92)90078-f. PubMed PMID: 1426532.
- 942 65. Pang YY, Schwartz J, Bloomberg S, Boyd JM, Horswill AR, Nauseef WM. Methionine sulfoxide
- 943 reductases protect against oxidative stress in Staphylococcus aureus encountering exogenous oxidants
- and human neutrophils. Journal of innate immunity. 2014;6(3):353-64. Epub 2013/11/20. doi:
- 945 10.1159/000355915. PubMed PMID: 24247266; PubMed Central PMCID: PMCPMC3972283.
- 946 66. Mashruwala AA, Pang YY, Rosario-Cruz Z, Chahal HK, Benson MA, Mike LA, et al. Nfu facilitates
- the maturation of iron-sulfur proteins and participates in virulence in *Staphylococcus aureus*. Mol
- 948 Microbiol. 2015;95(3):383-409. doi: 10.1111/mmi.12860. PubMed PMID: 25388433.
- 949 67. Kreiswirth BN, Löfdahl S, Betley MJ, O'Reilly M, Schlievert PM, Bergdoll MS, et al. The toxic shock
- 950 syndrome exotoxin structural gene is not detectably transmitted by a prophage. Nature.
- 951 1983;305(5936):709-12. doi: 10.1038/305709a0.
- 952 68. Novick RP. [27] Genetic systems in Staphylococci. Methods in enzymology. 204: Academic Press;
- 953 1991. p. 587-636.
- 954 69. Price EE, Rudra P, Norambuena J, Roman-Rodriguez F, Boyd JM. Tools, Strains, and Strategies To
- 955 Effectively Conduct Anaerobic and Aerobic Transcriptional Reporter Screens and Assays in
- 956 Staphylococcus aureus. Appl Environ Microbiol. 2021;87(21):e0110821. Epub 20210818. doi:
- 957 10.1128/AEM.01108-21. PubMed PMID: 34406831; PubMed Central PMCID: PMCPMC8516040.
- 958 70. Patel JS, Norambuena J, Al-Tameemi H, Ahn YM, Perryman AL, Wang X, et al. Bayesian Modeling
- and Intrabacterial Drug Metabolism Applied to Drug-Resistant Staphylococcus aureus. ACS infectious
- 960 diseases. 2021;7(8):2508-21. Epub 2021/08/04. doi: 10.1021/acsinfecdis.1c00265. PubMed PMID:
- 961 34342426; PubMed Central PMCID: PMCPMC8591627.
- 962 71. Melamud E, Vastag L, Rabinowitz JD. Metabolomic analysis and visualization engine for LC-MS
- 963 data. Analytical chemistry. 2010;82(23):9818-26. Epub 2010/11/06. doi: 10.1021/ac1021166. PubMed
- 964 PMID: 21049934; PubMed Central PMCID: PMCPMC5748896.
- 965 72. Price EE, Rudra P, Norambuena J, Román-Rodríguez F, Boyd JM. Tools, Strains, and Strategies To
- 966 Effectively Conduct Anaerobic and Aerobic Transcriptional Reporter Screens and Assays in

- Staphylococcus aureus. Appl Environ Microbiol. 2021;87(21):e01108-21. doi: doi:10.1128/AEM.01108-968 21.
- 969 73. Mashruwala AA, Boyd JM. The Staphylococcus aureus SrrAB Regulatory System Modulates
- 970 Hydrogen Peroxide Resistance Factors, Which Imparts Protection to Aconitase during Aerobic Growth.
- 971 PLoS One. 2017;12(1):e0170283. Epub 2017/01/19. doi: 10.1371/journal.pone.0170283. PubMed PMID:
- 972 28099473; PubMed Central PMCID: PMCPMC5242492.
- 973 74. Rosario-Cruz Z, Eletsky A, Daigham NS, Al-Tameemi H, Swapna GVT, Kahn PC, et al. The copBL
- operon protects Staphylococcus aureus from copper toxicity: CopL is an extracellular membrane—
- 975 associated copper-binding protein. Journal of Biological Chemistry. 2019;294(11):4027-44. doi:
- 976 https://doi.org/10.1074/jbc.RA118.004723.
- 977 75. Parker D. CD80/CD86 signaling contributes to the proinflammatory response of Staphylococcus
- 978 aureus in the airway. Cytokine. 2018;107:130-6. doi: 10.1016/j.cyto.2018.01.016. PubMed PMID:
- 979 29402722; PubMed Central PMCID: PMCPMC5916031.
- 980 76. Fey PD, Endres JL, Yajjala VK, Widhelm TJ, Boissy RJ, Bose JL, et al. A genetic resource for rapid
- and comprehensive phenotype screening of nonessential *Staphylococcus aureus* genes. mBio.
- 982 2013;4(1):e00537-12. Epub 2013/02/14. doi: 10.1128/mBio.00537-12. PubMed PMID: 23404398;
- 983 PubMed Central PMCID: PMC3573662.
- 77. Tan X, Ramond E, Jamet A, Barnier J-P, Decaux-Tramoni B, Dupuis M, et al. Transketolase of
- 985 Staphylococcus aureus in the Control of Master Regulators of Stress Response During Infection. The
- 986 Journal of Infectious Diseases. 2019;220(12):1967-76. doi: 10.1093/infdis/jiz404.
- 987 78. Winston F, Dollard C, Ricupero-Hovasse SL. Construction of a set of convenient Saccharomyces
- cerevisiae strains that are isogenic to S288C. Yeast. 1995;11(1):53-5. Epub 1995/01/01. doi:
- 989 10.1002/yea.320110107. PubMed PMID: 7762301.
- 990 79. Bose JL, Fey PD, Bayles KW. Genetic tools to enhance the study of gene function and regulation
- in Staphylococcus aureus. Appl Environ Microbiol. 2013;79(7):2218-24. Epub 2013/01/29. doi:
- 992 10.1128/AEM.00136-13. PubMed PMID: 23354696; PubMed Central PMCID: PMC3623228.
- 993 80. Forsyth RA, Haselbeck RJ, Ohlsen KL, Yamamoto RT, Xu H, Trawick JD, et al. A genome-wide
- strategy for the identification of essential genes in *Staphylococcus aureus*. Mol Microbiol.
- 995 2002;43(6):1387-400. PubMed PMID: 11952893.

- 996 81. Schneewind O, Model P, Fischetti VA. Sorting of protein A to the staphylococcal cell wall. Cell.
- 997 1992;70(2):267-81. doi: 10.1016/0092-8674(92)90101-h. PubMed PMID: 1638631.
- 998 82. Luong TT, Lee CY. Improved single-copy integration vectors for *Staphylococcus aureus*. J
- 999 Microbiol Methods. 2007;70(1):186-90. Epub 2007/05/22. doi: S0167-7012(07)00137-6 [pii]
- 1000 10.1016/j.mimet.2007.04.007. PubMed PMID: 17512993; PubMed Central PMCID: PMC2001203.